MACH "Y" STEMS FROM SPHERICAL SHOCKS

DWIGHT W. GLENN
and
ROBERT S. SALIN

UNITED STATES
NAVAL POSTGRADUATE SCHOOL

THESIS

MACH "Y" STEMS FROM SPHERICAL SHOCKS

Photo Investigation of the
Effects of Fractional Gram Charges

by

Dwight W. Glenn, 1st Lt, U.S.A.
and
Robert S. Salin, Lt, U.S.N.

1960

12ND P2238 (1-59)

MACH "Y" STEMS FROM SPHERICAL SHOCKS

Photo Investigation of the Effects of Fractional Gram Charges

by

Dwight W. Glenn

First Lieutenant, United States Army

and

Robert S. Salin

Lieutenant, United States Navy

Submitted in partial fulfillment of
the requirements for the degree of

MASTER OF SCIENCE
IN
PHYSICS

United States Naval Postgraduate School
Monterey, California

1960

MACH "Y" STEMS FROM SPHERICAL SHOCKS

Photo Investigation of the Effects of Fractional Gram Charges

* * * * *

Dwight W. Glenn
and
Robert S. Salin

MACH "Y" STEMS FROM SPHERICAL SHOCKS
Photo Investigation of the Effects of Fractional Gram Charges

by

Dwight W. Glenn

and

Robert S. Salin

This work is accepted as fulfilling
the thesis requirements for the degree of
MASTER OF SCIENCE
IN
PHYSICS
from the
United States Naval Postgraduate School

ABSTRACT

An investigation of primary and reflected spherical shock wave phenomena was conducted by center-detonating spherical $\frac{1}{4}$ gram PETN (Penta-erythritol tetranitrate) charges and photographing the resulting shock waves. This was done at accurately timed intervals in the range of 40 to 1000 microseconds with a Polaroid camera in conjunction with a high intensity xenon flash tube as a light source.

Clear and measureable photographs of the primary and reflected shock waves with associated Mach stem formation were obtained over the entire range of investigation.

Since this paper represents the first data ever obtained on a laboratory scale of Mach stem phenomena, correlation of spherical shock wave parameters was necessarily made with available theoretical and experimental data by using primary shock wave data.

Correlation results were excellent which shows that the Mach stem and other data contained herein are accurate and therefore reliable in determining high yield shock wave parameters by the use of appropriate scaling.

ACKNOWLEDGEMENT

The assistance and encouragement of Professors G. F. Kinney, J. F. Sinclair, J. W. Wilson, A. R. Frey, F. L. Coonan, Captain R. E. Odening and ET-1 R. Overlock are gratefully acknowledged.

Further, the technical support and assistance of the Postgraduate School Machine Shop, Photographic Laboratory, and the technicians of the Engineering School Physics Department were invaluable in the successful completion of this project.

TABLE OF CONTENTS

LIST OF ILLUSTRATIONS

TABLE OF SYMBOLS AND ABBREVIATIONS

a	cm/sec	Speed of sound under prevailing ambient conditions
ΔA	ergs	Calculated energy of explosion
D_{tp}	cm	Horizontal distance from ground zero (point on blast table directly above charge) to triple point
D_y	cm	Horizontal distance from ground zero to Mach stem (Mach "Y")
M	dimensionless	Mach number
P_o	dyne/cm^2	Atmospheric pressure in undisturbed air under prevailing ambient conditions
ΔP	atmospheres	Peak overpressure
p	atmospheres	Overpressure
H_{tp}	cm	Height of triple point from blast table
R_p	cm	Radius of primary shock wave
R_r	cm	Radius of reflected shock wave
t	microseconds	Delay time or arrival time of shock wave at an observed radius
t_a	microseconds	Arrival time of sound wave at an observed radius (under prevailing ambient conditions)
W	grams	Charge weight
PETN		Pentaerythritol tetranitrate
TNT		Trinitrotoluene
α	cm	Reduced energy parameter
λ	dimensionless	Reduced radius parameter
τ	dimensionless	Reduced time parameter

1. Introduction

Measurements obtained from microscale explosions have proved to predict accurately, the primary shock parameters of high yield explosions where properly scaled. Of significance is the time of arrival-overpressure relationship which, due to exactness in electronic timing devices, is more desirable than the usual inexactness of pressure gage instrumentation encountered in field tests.

Since reflection parameters from decigram charges bear a direct relationship to reflection parameters encountered in conventional and atomic explosions, this project endeavored to establish decigram reflection data for scaling purposes. In particular, the accurate determination of Mach stem formation and associated reflected data in field tests is not only expensive but the tests themselves cannot be carried out under all field conditions, i.e., controlled factors, and for this reason the accomplishment of such measurements on a decigram scale is very useful.

2. Electronic Circuitry and Determination of Time Delay

The electrical and electronic circuitry of this experiment had three functions: First, to initiate the PETN charge electrically; second, to provide a time delay between the instant of explosion and the xenon flast tube reaction; and third, to provide a precise means of measuring the time delay between the instant of explosion and the xenon flash tube reaction.

(1) Firing Circuit. Since the decigram explosive chain starts by heating the lead styphnate detonator, it was correctly assumed that satisfactory initiation could be obtained by passing a high enough current through the detonator wire used in the charges.

Initially, a circuit configuration as shown in Fig. 5 was used. This firing circuit gave reliability of detonation but was found to be hazardous due to the high voltage condensor. A second method was used which was found to be nearly as reliable as well as simple and very safe. This firing circuit is shown in Fig. 3a.

It consisted of a 110 volt AC supply (wall outlet), a variac and a firing switch. It was found by trial that 30 volts could be used reliably to detonate the charge with the added feature of a second break in the firing circuit, provided by the variac "off" switch, while mounting a subsequent charge under the blast table. This added safety feature outweighed other considerations.

The reduction of firing voltage to 30 volts raised

the question as to how much delay would exist between the instant of explosion and the instant the No. 1 photocell would detect the explosion. The question was resolved by mounting a charge and firing it with the firing key triggering the time base of a type 515A oscilloscope while running the photocell output to the vertical input of the oscilloscope. A picture was taken of the scope trace by a Polaroid mount at the instant of explosion which showed an instantaneous reaction of the photocell. It was concluded, therefore, that the reduced voltage caused negligible time delay between keying and photocell pick-up.

(2) Photographic Delay Circuit. Once the means of actually detonating the charge was resolved, it was necessary to provide a measureable time delay between inception of explosion and the instant a picture was taken of the propagating shock front. The problem here was actually twofold: (a) How to take a picture of the explosive shock wave; and, (b) how to take this picture at a measured instant of time (in microseconds) after the explosion had occurred.

The first problem was resolved by mounting the charge in front of a white, reflective background. The camera shutter was opened and the charge detonated in quick succession. Shortly thereafter, a xenon flash tube, mounted next to the camera, flashed, and this flash of intense light cast a shadow of the shock wave on the white background. A photograph of the shock wave resulted.

The measureable time delay between explosion and xenon flash was accomplished by using the circuitry of Fig. 3b.

Photocell No. 1, utilizing an RCA 868 photocell tube, sensed the instant of explosion and transmitted this pulse simultaneously to (1) a Hewlett Packard electronic counter and (2) a General Radio pulse, sweep and time delay generator. The delay generator delayed the incoming pulse a pre-selected amount of time (calibrated dial settings of the delay generator varied from one microsecond to one second). The delay generator output, as shown in Fig. 3b, was then transmitted to the xenon circuit. This pulse closed a thyratron electronic switch, causing a pre-charged condensor to discharge 1200 volts through the xenon tube which then fired. Pre-selected times between explosion and xenon flash were obtained by merely varying the above mentioned dial.

(3) Time Measurement Circuit. The problem of time measurement was basically to measure as accurately as possible, the time increment, in microseconds, between inception of explosion and xenon flash (when picture of shock wave was taken). This was done by using the circuitry of Fig. 3c. At the instant an explosion occurred, photocell No. 1 transmitted a pulse to a Hewlett-Packard counter, Model FR-38A/U. This pulse started the device counting in tenths of microseconds. At the instant the xenon flash occurred, photocell No. 2 generated a pulse and transmitted this pulse to the electronic counter's stop trigger. Thus, photocell No. 1 started the counter at the instant of detonation; photocell No. 2 stopped the counter at the

instant the xenon flashed. The counter was then read and recorded to the nearest tenth of a microsecond for each shot.

Initially, it was planned to use one photocell to detect the explosion and transmit a pulse to the delay generator; the generator would send a pre-set delayed pulse to the xenon circuit. Ideally, the total time delay would be that set on the dial of the delay generator. This simple plan proved unacceptable for several reasons. First, the delay generator time delay was determined to be in error. This error was observed by using a pulse generator and a 515A oscilloscope. An input pulse from the pulse generator was run into the input side of the delay generator and simultaneously to the "external synch" of the scope. The output of the delay generator was lead to the vertical input of the scope. Thus, the vertical pulse appearing on the scope sweep was an accurate measure of the delay generator time delay. At a setting of 600 microseconds on the delay generator, the scope indicated an actual delay of 620 microseconds. A 20 microsecond error was unacceptable even though considerably less error was observed at low time delay settings.

A second reason for rejecting the single photocell circuit was due to an inherent delay in the photocell-delay generator circuit. This could only be understood by noting that the input triggering level of the delay generator had a minimum of approximately ten volts. This meant that an additional time increment was added to the delay time,

commensurate with the length of time it took the photocell pulse to rise to at least ten volts. The photocell rise time was determined to be relatively long which meant that the time increment error was unacceptably large. The photocell rise time was determined by using a strobotac in conjunction with the 515A oscilloscope. While the strobotac pulsed the photocell at the rate of about 60 times per second (line position), the strobolux was used to trigger externally, the scope sweep. In this manner an accurate picture of the photocell rise time was obtained.

Subsequently, it was determined to build a photocell unit with an extremely fast rise time in order to eliminate this hidden error. Both photocells were configured as shown in Fig. 4. Note that the photocell provides positive grid bias to a simple cathode-follower. This cathode-follower amplifier was particularly suited to the needs of the experiment since its output pulse is inherently of an extremely short rise time duration.

A third major draw-back to the use of an "ideal" delay generator circuit for xenon flash and time measurement was found to be the xenon circuit itself. It was found that the inherent time delay of the xenon circuit, i.e., the time between input pulse and actual xenon flash, varied between 30 and 60 microseconds. This xenon circuit time delay was determined by sending a pulse to the xenon circuit input and simultaneously to the "external synch" of the 515A oscilloscope. A photocell was placed in front of the xenon

tube and its output became the vertical input of the scope. Thus, the scope sweep gave an accurate measure of the time delay of the xenon circuit.

Subsequently the photocell was replaced by a "noise" wire in the above determination of xenon circuit delay. This noise wire consisted of a co-axial line with one end bared and wrapped several times around the middle of the xenon tube. The other end was the vertical input to the scope. When the pulse generator pulsed the xenon circuit, the xenon tube fired; the ionization within the tube generated a voltage in the noise wire which caused a pulse on the scope sweep. As expected, this pulse position coincided almost exactly with that of the photocell pulse when the xenon tube flashed. The interesting thing about the noise pulse was that it indicated the xenon tube intensity pattern was about three microseconds for a 1/3 peak duration. This observation coincided exactly with the FX-11 xenon tube manufacturer's specification.

In summary, it was determined that the use of an idealized delay generator circuit for production and measurement of time delay was inadequate because, (a) there was an inherent time delay error in the photocell circuit due to a minimum triggering level input to the delay generator; (b) the delay generator dial was inaccurate; (c) there existed an inherent time delay in the xenon circuit of a measureable but unpredictable amount; (d) there existed a time increment in the intensity of the xenon flash pattern which gave an error of ± 1.5 microseconds.

Although this idealized delay generator circuit proved unsatisfactory, it was highly useful in a systematic analysis of the circuitry in order to discover and eliminate possible errors in the measurement of the time delay used. This discussion was included here as a possible guide to future time delay problems in this field.

A chronological resume' of the system is as follows: (Refer to Fig. 3a,b,c). Immediately after the camera shutter was opened the firing key was closed and the explosion occurred. Photocell No. 1 transmitted this pulse to the electronic counter (start). The delay generator transmitted a delayed pulse, pre-selected, to the xenon circuit. (All transmission delays are short enough to be neglected.) The delayed pulse activated a thyratron switch which allowed a capacitor to discharge into the xenon tube. The xenon tube flashed and a picture of the shock wave was taken at that instant. Also at the instant of flash, photocell No. 2 sent a pulse to the electronic counter (stop).

Time error here was determined to be ± 1.5 microseconds due to the 1/3 peak duration of the xenon tube as previously described. Again, due to the extremely fast rise time of the photocell and low triggering level of the counter, the time error of transmission between these two units was negligible.

The electronic counter was designed and calibrated to be accurate to two parts in one million; therefore, the total error was estimated to be approximately two microseconds.

The time indicated on the electronic counter measured the time between inception of the explosion and the instant of xenon flash.

Shielded leads were used throughout the circuitry to eliminate possible interference noise between one component and another, particularly the xenon capacitor discharge circuit.

3. Preparation of Detonators and Charges

Since it had been shown that PETN, with lead azide and lead styphnate detonators, was well suited for studies of this nature (Ref. 1), it was decided to duplicate this method of preparation of charges, utilizing approximately 0.3 grams of PETN. It was determined, however, that a slight reduction in the amount of PETN (to 0.25 grams) resulted in easier preparation and a lower percentage of duds without any apparent change in the resultant shock phenomena with the exception of the loss in energy attributable to the 0.05 gram PETN reduction.

The PETN utilized was procured from the Trojan Powder Co., Allentown, Penna.; the lead azide and lead styphnate were available in the explosives laboratory of the Chemistry Department, U. S. Naval Postgraduate School.

The method of detonator preparation described by Reference 1 was found to be too time consuming and resulted in faulty detonators some of the time. A quicker method which gave only one or two faulty detonators out of several hundred was as follows:

a. Fuse wire, 15 cm. in length was used. (Standard fuse wire used in oxygen bomb calorimetry.)

b. A simple over-hand knot was tied in the center of the wire, resulting in a small loop.

c. The size of the loop was adjusted by merely pulling on the ends of the wire. The final size was adjusted to one to one and a half millimeters in diameter.

[illegible]

[illegible]

[illegible]

[illegible]

[illegible]

[illegible]

[illegible]

d. From 50 to 100 loops were formed before proceeding.

e. Approximately $\frac{1}{2}$ gram of lead styphnate was placed on a watch glass and covered with acetone. Several drops of Duco cement were added to the styphnate and mixed with the square-ended brush until a proper consistency was obtained. A "proper consistency" was one that allowed the mixture, when applied to the loop, to adhere.

f. It was usually necessary to add acetone to the mixture to keep the same consistency.

g. Upon obtaining this consistency, the brush was used to scoop up the mixture which was then deposited on the loop. A slight pause between watch glass and loop allowed some acetone to evaporate and made application easier. An air hose or blowing by mouth on the bead facilitated drying before proceeding to the next loop. After applying the styphnate to the 50-100 loops, they were left uncovered over night to allow all the acetone to evaporate.

h. After the styphnate beads were dried, lead azide was treated in the same manner, i.e., watch-glass, Duco cement, etc., and then carefully coated over the styphnate bead. Too much acetone on the brush loosened the styphnate bead causing it to drop off or it wetted the styphnate sufficiently to cause an azide-styphnate mixing. The latter apparently happened if the bead turned a reddish color and was cause for rejection. However, these were rare occurrences and very few faulty detonators occurred. The lead azide process was laborious, but rightly so-complete and even application was necessary to form good detonators.

i. One additional procedure used was: Upon obtaining the size loop desired (before styphnate application), a pair of needle-nosed pliers was used to squeeze the loop flat so there would be less "give" to the loop while handling. Centering the loop in the pliers towards the larger end of the pliers resulted in right-angled bends near the loop, providing the ends of the wire were pulled correctly. These right-angled bends facilitated placement of the detonator in the charge die base.

Fig. 7 shows the various stages in detonator and charge preparation.

The acetone in detonator preparation served a dual purpose; it desensitized the explosives while mixing etc., and served as a medium for wetting the powdered explosives to allow for application. Since sufficient drying allowed for complete evaporation of acetone, its initial presence had no effect on the end results.

The Duco cement served one purpose only-that of having an adhesive agent for the powdered explosives. Although the dried cement remained part of the detonators, any additive or deleterious effects were neglected.

The preparation of charges was as follows:

a. 0.25 grams of PETN were placed on watch-glasses.

b. With the die body and base properly placed together, a funnel was inserted in the bore. Approximately one third of the PETN was placed down the bore.

c. Upon removal of the funnel a brass plunger was

[illegible]

[illegible]

[illegible]

[illegible]

[illegible]

[illegible]

[illegible]

inserted and the PETN was lightly tamped down, forming a hemisphere in the die base.

d. The die body was then removed, the base being inserted in a vise (to allow for easier handling). While in this position, the detonator wires were pulled through the small holes in the base, the right-angled bends being placed at the top of the base grooves. Pulling the wires taut from the bottom allowed the die body to be placed back in position over the die base. It was necessary that the body be flush to the base or an excess amount of PETN was lost or else the pressing of the charge would fail.

e. After removal from the vise the funnel was again inserted and the remaining PETN deposited down the bore.

f. A small amount of powdered graphite was placed in the hemispherical end of the plunger which was then placed down the bore. A collar was fitted between the plunger cap and die body to prevent excess pressure from being exerted.

g. The die was placed in the press such that pressure would be exerted straight down on the plunger. Pressure was applied on the plunger until such time the press could not be easily turned by hand. (The collar remained free of pressure while in place).

h. Upon removal of the die from the press, the collar was removed and the plunger lifted directly up until lodged in the bore. Compressed PETN along the sides of the plunger usually prohibited the plunger from being lifted up all the way without force.

i. With the plunger lodged in the bore (free from the charge) the die body was separated from the base by a direct lifting action, leaving the charge affixed in the die base.

j. By giving a quarter-turn of the screw on the underside of the base with an allen wrench, the charge was freed from the base. Pushing the wires from the underside allowed for easy extraction. The charge was then placed in a dessicator until needed for detonation.

The utilization of graphite, the effects of which are neglected in detonation, allowed easier separation of the charge from the plunger upon extraction. Without the use of graphite, hemispherical charges resulted. Also, after several pressings, the plunger "belled-in" and necessitated "belling-out" by placing it over a ball bearing of correct dimensions and tapping lightly several times. Without this "belling-out", the plunger would pull the charge in half.

Although 0.25 grams were weighed, a small portion, approximately 0.006 grams, was lost each time. A standard procedure minimized the loss and deviations therefrom.

Fig. 8 shows the equipment necessary for charge and detonator preparation.

4. Experimental Setup

The experimental setup consisted of the following basic components:

a. Delay generator
b. Xenon tube and associated electronic circuit
c. Two photocells
d. Hewlett Packard electronic counter
e. Model 110A Polaroid camera
f. 120 volt variac and firing key with associated wiring
g. Horizontally mounted aluminum blast table
h. Various shielded leads connecting the components
i. One optical telescope providing cross-hair alignment
j. One Scotch-Lite grid screen

Fig. 8 shows the integrated configuration of these basic components.

The Scotch-Lite screen was mounted on the wall and firmly held in place by the heavy blast table. Grid wires were criss-crossed at measured ten centimeter intervals on the screen to provide a means of measuring the position of the shock wave in the photographs.

An aluminum blast table measuring 133 x 111 x 0.8 cm. was elevated a distance of 84.5 cm. above the assembly table and held in position by four metal posts C-clamped to the table. The plate was center-drilled a distance of 60 cm. from the grid screen to receive the firing circuit wire ends to which the charge was attached.

One photocell unit was clamped to a blast table support

[illegible]

[illegible]

[illegible]

[illegible]

[illegible]

posts and carefully oriented in height and azimuth to insure proper photocell sensing direction.

Mounted on a wooden frame on the assembly table, 300 cm. from the grid screen, was the Polaroid camera. Type 44, 400 ASA Polaroid film was used throughout the experiment.

With the charge mounted 60 cm. from the screen and the camera lens mounted 300 cm. from the screen, the shock wave projection was dimensionally augmented by a factor of 1.25. For this reason, all parameters measured on the photographs were divided by 1.25 to correctly place the measurements in the plane of the charge and not in that of the grid screen.

Mounted on the wooden frame directly beneath the camera lens was the Edgerton, Germhausen, and Grier FX-11 xenon flash tube. This tube was rated at one candlepower with one third peak duration of three microseconds. The tube was contained in a foil lined cylindrical container, the foil giving reflection and increased intensity. A small hole was drilled in the front of the container facing the charge to serve as an aperture. This aperture was approximately one sixteenth of an inch in diameter which made the xenon tube an effective point source of light.

Situated on a stand adjacent to the xenon tube was the second photocell unit. This unit was also made highly directional to eliminate stray light interference; this unit was pointed directly at the xenon flash tube.

The associated electronic equipment to give the xenon tube a required 1200 volts potental was mounted on top of

the wooden frame housing the camera. This component consisted essentially of an electronic thyratron switch which, when closed by a pulse from the delay generator, allowed a 1.75 microfarad capacitor to discharge across the flash tube. An auxiliary circuit and toggle switch were also a part of this unit to provide a means of test firing the xenon tube for alignment prior to each shot.

As shown in Fig. 9, the bottom of the wooden frame housed the delay generator and its associated power unit. Beside this was the Hewlett Packard electronic counter.

The start input of the counter was connected by a shielded lead to the "direct synch out" of the delay generator. The stop input of the counter was similarly connected to the photocell mounted at the xenon flash tube.

The other photocell (at the blast table) was connected directly to the "PRF drive (input)" of the delay generator.

The delay generator's "delay synch out" was connected to the xenon tube's electronic control box.

At the extreme opposite end of the assembly table, a cross-hair telescope was mounted on a stand. The cross-hairs were situated precisely 79.5 cm. above the table and in direct line with the center of the camera lens and the screen's center grid intersection, five centimeters below the blast table. Prior to each shot the charge was mounted and adjusted until the cross-hairs intersected the center of the spherical charge. In this manner, each charge was placed in the same position each time, exactly five

centimeters below the blast table, directly in front of the central grid intersection of the screen. A meter stick was used to ascertain the proper distance from the grid screen.

Other auxiliary equipment used were instruments for measuring the ambient temperature, pressure and relative humidity; a traveling microscope (with altered objective lens) was used for the measurement of the photographs.

5. Experimental Procedure

The experiment was conducted in two phases. First, the photographing of the shock wave at various time intervals from instant of explosion out to approximately 1000 microseconds. Second, the measurement of the various parameters associated with the reflected shock waves from the photographs obtained during the first phase. This measuring procedure was done with a traveling microscope rig that allowed exact measurements (within resolving limits).

Initially a charge was attached to the firing circuit wire ends under the blast table. It was then adjusted to intersect with the telescope cross-hairs. This placed the charge five centimeters below the blast table and precisely on the centerline of the camera lens and xenon tube for each shot. A meter stick was used to insure that the charge was also situated 60 cm. from the grid screen.

The xenon tube was then test fired with the control box toggle switch in order to adjust the xenon aperture and center the light intensity pattern on the screen. This was necessary prior to each shot since, for increasing time delay intervals, the intensity pattern had to be placed lower in order to insure a strong reflection of the larger primary and reflected shock wave radii.

An appropriate time delay was selected and introduced into the system by adjusting the time delay dial on the face of the delay generator.

Since the inherent time delay of the xenon circuit was known to be from 30 to 60 microseconds, a correction factor of approximately 40 microseconds was introduced into the dial setting. Because the xenon circuit delay was so unpredictable, the total time delay could never be predicted accurately in advance although this was unimportant because of the extremely accurate time measurement of the actual shot. Over the range between 40 and 1000 microseconds, 42 of the shots fired were selected to give adequate coverage.

After completing the time delay adjustment, the camera was cocked and mounted directly over the xenon flash tube aperture after which the variac was adjusted to 30 volts and then turned on.

To accomplish the actual firing and photographing, the camera shutter was opened manually immediately followed by depression of the firing key which set off the explosive charge.

The camera shutter was released thereafter and the variac zeroed and turned off before mounting a subsequent charge. (The latter procedure was a safety precaution).

The actual time delay was read from the counter indicator and recorded after each shot.

After the photographs were developed they were placed under the traveling microscope where each parameter was measured twice, averaged, and recorded.

6. Data

Basic data obtained from experimental procedure is included as Table 1. Values not shown (where applicable) were due to the inability to measure the parameters on the photographs (obliteration, etc.). Tabulated below are values for: t, delay time; R_p, primary radius; R_r, reflected radius; H_{tp}, height of triple point; D_y, distance to Mach stem; D_{tp}, distance to triple point.

Table 1

No. Shot	t(μsec)	R_p(cm)	R_r(cm)	H_{tp}(cm)	D_y(cm)	D_{tp}(cm)
1	45	5.8				
2	78	9.1				
21	79	10.0				
22	100	10.6				
23	124	12.1		2.6	13.8	11.8
24	141	13.4				
36	146	13.9		2.7	15.2	13.6
39	162	14.2	9.9	3.9	17.1	14.1
88	168	14.3	10.6	4.3	16.9	14.3
89	179	15.2		4.5	17.5	15.2
41	186	15.7	11.5	4.6	17.8	15.7
16	198	16.0	11.6	4.6	18.1	15.9
20	198	16.0	11.4	4.6	18.0	15.9
42	218	16.4	12.8	6.4	18.7	16.4
43	228	17.4	13.3	7.1	20.0	17.2
90	240	17.3	13.6	6.6	20.9	16.9
68	241	18.2	13.8	6.8	20.6	18.1

No. Shot	t(μsec)	R_p(cm)	R_r(cm)	H_{tp}(cm)	D_y(cm)	D_{tp}(cm)
44	266	19.9		7.2	21.9	19.8
47	282	20.1	15.3	7.8	22.7	20.0
48	306	20.9		9.3	24.1	20.4
49	336	22.1	18.6	12.0	25.3	21.0
50	356	22.9	19.0	12.7	26.4	21.6
81	372	24.9	20.0	12.0	27.0	23.9
51	378	24.0	20.0	11.7	27.2	23.0
74	381	24.8	19.4	10.8	26.8	24.1
53	396	24.8	21.1	12.5	28.0	23.7
57	420	25.8	22.1	15.2	27.7	23.7
59	444	26.2	23.1	14.8	29.6	23.8
70	446	26.3	22.1	15.1	30.2	25.4
72	448	27.3	22.9	15.1	29.4	24.2
63	462	27.8	23.5	15.3	31.0	25.8
65	482	29.2	24.7	14.5	31.4	27.6
78	483	28.8	24.0	16.5	31.8	26.5
80	493	28.7	25.9	18.0	32.4	25.7
76	523	30.0	25.4	17.7	33.4	27.2
66	528	30.6	26.2	17.0	33.6	28.2
79	560	30.6	27.8	19.6	35.0	26.8
82	592	33.4	29.0	19.6	36.4	30.0
62	725	38.8	34.7	26.8	42.0	32.2
60	763	40.3	35.5	27.6		33.2
67	800	41.2		26.2	45.9	35.0
73	859	44.4			47.2	

7. Computational Procedure

A. Parameters assumed constant.

1. Temperature: The weighted average observed temperature was 72°F. Since tabular data was available using 70°F, the difference was considered negligible and a value of 70°F was used as the ambient temperature.

2. Pressure (P_o): The weighted average pressure was 765mm. Hg. Since tabular data was available for calculations involving 760 mm. Hg., five millimeters Hg. was considered negligible and a value of 760 mm. Hg. (14.7 psia) was taken as ambient pressure. In the c.g.s. system, this converts to a value of approximately 1.02×10^6 dynes/cm^2.

3. Charge configurations:

(a) Shape: spherical, diameter of 0.706 cm.

(b) Density: loading density of 1.5 gm/cm^3.

(c) Weight: 0.244 gm. PETN, 0.003 gm. lead styphnate, 0.010 gm. lead azide and 0.022 gm. of fuse wire.

4. Geometry of experiment:

(a) Charge height (vertical distance below blast table): five centimeters.

(b) Grid distances: ten centimeters by ten centimeters per grid. Since the grid was made by stretching black nylon thread over a reflective screen, there was a slight deviation from grid to grid but these deviations were minimized by measuring and readjusting before firing.

(c) Reducing factor: 1.25 (dimensionless). Since the shock waves photographed were in the plane of the screen

.2[illegible]

.08[illegible]

.103[illegible]

1.7[illegible]

it was necessary to reduce all measurements by this factor in order to have the measurements in the plane of the charge. By using similar triangles and a charge-to-screen distance of 60 cm., a camera-to-screen distance of 300 cm., a reducing factor of 1.25 is arrived at.

(d) Camera lens and light source: The light source aperture was four centimeters from the center of the camera and for a distance of 300 cm., this was sufficiently close enough to assume camera lens and light aperture to be a point source.

(e) Speed of sound at ambient conditions: 34,300 centimeter per second.

(f) Energy of explosion (ΔA): The energy of explosion is calculated to be 7.69×10^{10} ergs per gram of PETN. (See Appendix II, Ref. 1). Since the charges consisted of explosives other than PETN it was necessary to convert these explosives to PETN equivalents. (See Ref. 5). By Trauzel test, lead styphnate is rated as 40% TNT and lead azide as 39% TNT. Therefore, 0.003 grams of lead styphnate are equal to 0.0012 grams of TNT; 0.01 grams of lead azide are equal to 0.0039 grams of TNT. This gives a total of 0.0051 grams of TNT for the detonator. Also by Trauzel test, PETN is rated as 173% TNT. Hence, 0.0051 grams of TNT are equal to 0.00295 grams of PETN and adding the amount of PETN used, gives a total charge weight of 0.247 gms. of PETN. A value of 0.25 grams was considered within acceptable limits of error. This then gives the energy of explosion per charge to be 1.925×10^{10} ergs.

B. Calculations

To correlate the experimental data to theoretical considereations (Fig. 1, Ref. 2), it was necessary to convert to the reference parameters, i.e., ΔP and λ. (Refer to p. vi for the meaning of the symbols used herein).

Now $\lambda = \frac{R_p}{\alpha}$ and $\Delta P = \frac{p}{P_0}$ where $\alpha = \left(\frac{\Delta A}{P_0}\right)^{1/3}$ and p is found from tabular values. (See Ref. 3). The value of α, using the constants above, was found to be 26.6 cm. . Using different values of R_p then gave values for λ.

To obtain the values of p, it was convenient to introduce the Mach number, M, and a time interval, t_a, which is the time required for a sound wave to travel the same distance under prevailing ambient conditions. By definition, $t_a = \frac{1}{a}\int_0^{R_p} dR_p$ and $t = \frac{1}{a}\int_0^{R_p}\frac{1}{M}dR_p$. Subtracting the second from the first, one obtains: $t_a - t = \frac{1}{a}\int_0^{R_p}(1-\frac{1}{M})dR_p$ or $\frac{d(t_a-t)}{dR_p} = \frac{1}{a}\left(1-\frac{1}{M}\right)$. Solving for M, $M = \frac{1}{1-a\left[\frac{d(t_a-t)}{dR_p}\right]}$, where $\left[\frac{d(t_a-t)}{dR_p}\right]$ is the slope of the curve of $(t_a - t)$ versus R_p. The values for time of arrival of a sound wave at any observed radius was calculated by $t_a = \frac{R_p}{34300} \times 10^6$ where t_a is in microseconds.

Fig. 12a shows the plot of $(t_a - t)$ vs. R_p. It was convenient to plot the calculated slopes vs. R_p and obtain a second smooth curve. This is shown in Fig. 12b. The value of the slope at any given R_p was taken from the second smooth curve and the corresponding Mach number computed therefrom. With the values of the Mach numbers, the overpressure was

found from Table 1 of Reference 3. Where Mach numbers exceeded those tabulated, the overpressure was calculated from the formula, $p = \frac{7(M^2-1)}{6} P_o$.

For a given R_p therefore, a value was found for λ and ΔP, giving the experimental points and representative smooth curve shown in Fig. 13.

To make a space-time correlation with Fig. 4, Ref. 2, a conversion was made to reduced time, $\tau = \frac{at}{\alpha}$ which was plotted against the reduced radius, $\lambda = \frac{R_p}{\alpha}$. Then for a given R_p and corresponding t, the reduced parameters were calculated and plotted, Fig. 14 showing the resulting curve.

Scaled distances and scaled times were also calculated where the scaled distance, $\frac{R_p}{W^{1/3}}$, is found by dividing a given R_p by the cube root of the charge weight, i.e., $(.25)^{1/3}$ and the scaled time is found by dividing the arrival time by the same value, i.e., $\frac{t}{W^{1/3}}$. Fig. 15 shows the resultant curve.

8. Results

Photographs of the shock waves, by using a Polaroid camera and type 44, 400 ASA film, were clear and produced easily measureable radii and reflection parameters over the entire range of the investigation.

The parameters measured (see Fig. 2) were plotted as distance vs. time (Fig. 15-19). As would be expected, these curves show a smooth growth of the parameters with time. As explained in Appendix I, it was determined that the Mach stem began between 80 and 85 microseconds after the explosion. For this reason, several of the reflected parameters indicate an experimental point at zero distance.

Correlation was made with pertinent portions of Ref. 2 and establishes the reliability of the measurements made here. Peak over-pressure versus reduced radius data obtained in this ivestigation were plotted in Fig. 13 with excellent results, particularly in the mid region of the reduced radius. Deviations at low radii between the PETN data of this experiment and that of theoretical point-source results for an ideal gas are accounted for by noting that blast efficiency in real air is reduced by molecular dissociation and ionization at high temperatures near the source of the explosion. It is noted that correlation between TNT and PETN at low radii are outstanding. At high radii ($\lambda > 1$) the deviation from both the ideal gas curve and TNT is significant which indicates data from this investigation is inadequate in these higher ranges.

Probable cause for the deviation in this region can be attributed to the fact that there was a small but finite distance between camera lens and xenon aperture in the experimental setup. Measurement of large shock radii would then be subject to geometrical errors due to this finite distance. In addition, at large radii, the reducing factor of 1.25 does not place the measured radius in the plane of the explosion since the reflected shadow of the primary radius was made from the shock front that was not in the plane of the charge. These two factors together will then account for deviations at large radii but as explained previously, the geometry of the experiment was assumed constant.

Fig. 14 shows a correlation of the reduced radius vs. reduced time obtained in this investigation with that of Brodie in Reference 2. It is noted that slope correlation is excellent. Comparison with the Brodie curve indicated a constant error along a 45 degree line between corresponding points of the two curves. This implies a discrepancy in the value used for α which is the reducing factor. This is reasonable since $\alpha = \left(\frac{\Delta A}{P_0}\right)^{1/3}$ and ΔA, the energy of explosion, is somewhat arbitrary.

Fig. 15 shows a plot of scaled radius versus scaled time whereby correlation can be made with different charge weight of PETN. The curve of Fig. 10, Reference 1, is shown in comparison. It is believed that the deviation in the two curves is attributable to a time measurement

error incorporated in Reference 1. By comparing data from this experiment and that of Reference 1 there appears to be a constant time error of approximately 80 microseconds.

In summary, over-all correlation was excellent and showed definitely that the measured parameters of this investigation were accurate. Of particular significance is the fact that these results indicate that overpressures may be calculated from arrival time data without resorting to the inexactness of pressure measuring instruments. These results also bear out that photographic microscale charge techniques can economically and safely be used to determine, by proper scaling, high yield explosive parameters.

Accuracy of results: By rather detailed analysis as previously mentioned, it was determined that the maximum error in time measurement throughout the range of investigation was, plus or minus, two microseconds. Microscopic measurement of the photographic data was accurate to, plus or minus, five millimeters. Grid wire placement on the grid screen was estimated to be accurate to plus or minus one millimeter and that of charge height placement, plus or minus one and a half millimeters.

Appendix I

The information contained herein, although not a part of the basic experiment, is based on observations during different experimental procedures and techniques. A quantitative treatment would be inappropriate since phenomena observed were singular incidents or not pursued in a quantitative manner. However, this would not preclude quantitative treatment and mention is made of these observations for the information of those to follow in a like experiment.

A. Attenuation of reflected parameters by rigidity of the reflected surface: Reference is made to Fig. 1 or Fig. 11; sitting upon the blast table was a cylindrical object. The object was a solid piece of brass weighing approximately ten pounds, the object of which, was to depress the center section of the blast table such that the lowest point of the blast table in the photographs would be that portion above the charge. The weight remained in that position throughout the experiment except for one occasion when another weight was placed next to it. This additional weight was also approximately ten pounds and nine charges were fired with both weights on the blast table. After the resulting photographs were measured and the data plotted, it was found that, although these data give the same slope as the "one weight" data, an augmentation was made in the distance. For example, the height of the triple point, (H_{tp}), was approximately three centimeters greater at a given time interval. It would appear from the observation above that the reflected

parameters are augmented by this additional rigidity factor. Just what the relationship is was not pursued.

B. Detonator size for greater charge weight: Although 0.25 gram charges were used for the experiment, a larger die was available for pressing a larger charge. This die would accomodate, approximately, a 0.50 gram charge. It was thought that the detonators prepared for the smaller charges would also suffice for a 0.50 gram charge. It was found, however, that the amount of lead azide used had to be at least tripled before the larger charge would detonate. Since this meant a larger detonator, the charge was reduced to 0.45 grams for successful firing.

C. Close-up photography: The Polaroid camera used had, as accessories, close-up lens. With the proper lens in place, the camera was moved to approximately 18 inches from the screen. (The charge was moved to approximately four inches from the screen). With the knowledge from previous photographs as to where the triple point was located for a given time delay, the camera was placed for that given location and the charge fired. Ten shots were successful at this range and greatly magnified the Mach stem formation in the photographs. By this method it was found that the Mach stem originated between 80 and 85 microseconds after detonation.

Also, as shown in Fig. 20a, an additional shock phenomena was observed. This was the "slip-stream" which was clearly discernible on one of the photographs.

D. Surface splitting of the Mach stem and internal reflection of the reflected shock wave: Fig. 20 b, a

drawing of a photograph, shows several interesting phenomena.

The first of these is an apparent splitting of the Mach stem at the surface of the blast table. No claim is being made that splitting actually occurred but probably due to some factor, e.g., geometrical, it appears as though splitting did occur.

Another interesting phenomena was the reflection (?) of the reflected wave inside the primary shock wave. An early attempt at mounting the charges involved a hollow brass tube, O.D. 5/16 inch, with the firing wires coming up through the tube which was mounted firmly upright. In this particular shot, the reflected wave appears to have been reflected from this tube as it progressed outward toward the primary shock. Whether or not this was actually the case was not ascertained.

Also in this shot, the secondary shock wave was clearly visible. It has been shown (Reference 1) that by other photographic equipment, the secondary shock wave is clearly visible in the time range of this experiment. The Polaroid camera was not optically suited for quantitative study of the secondary shock wave although it appeared in several of the photographs.

Figure 1

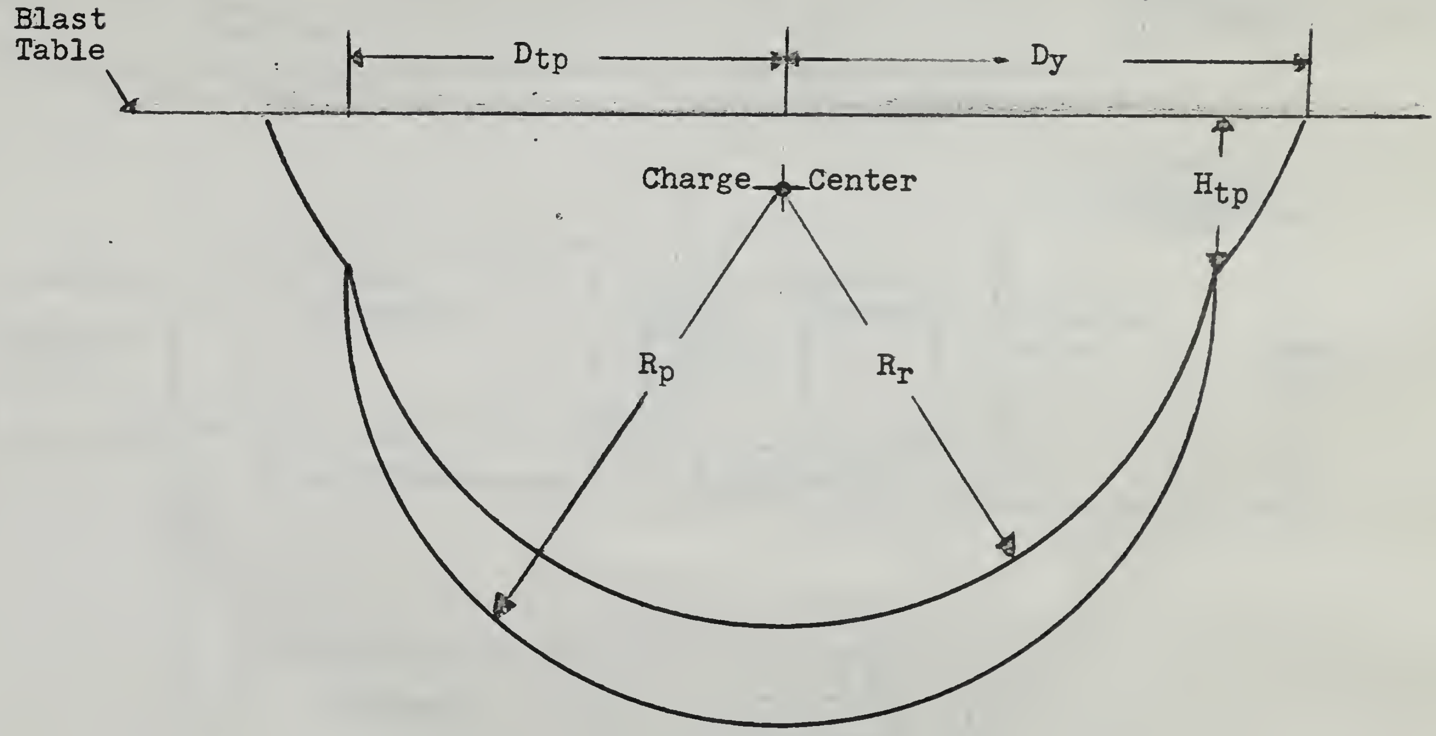

Figure 2

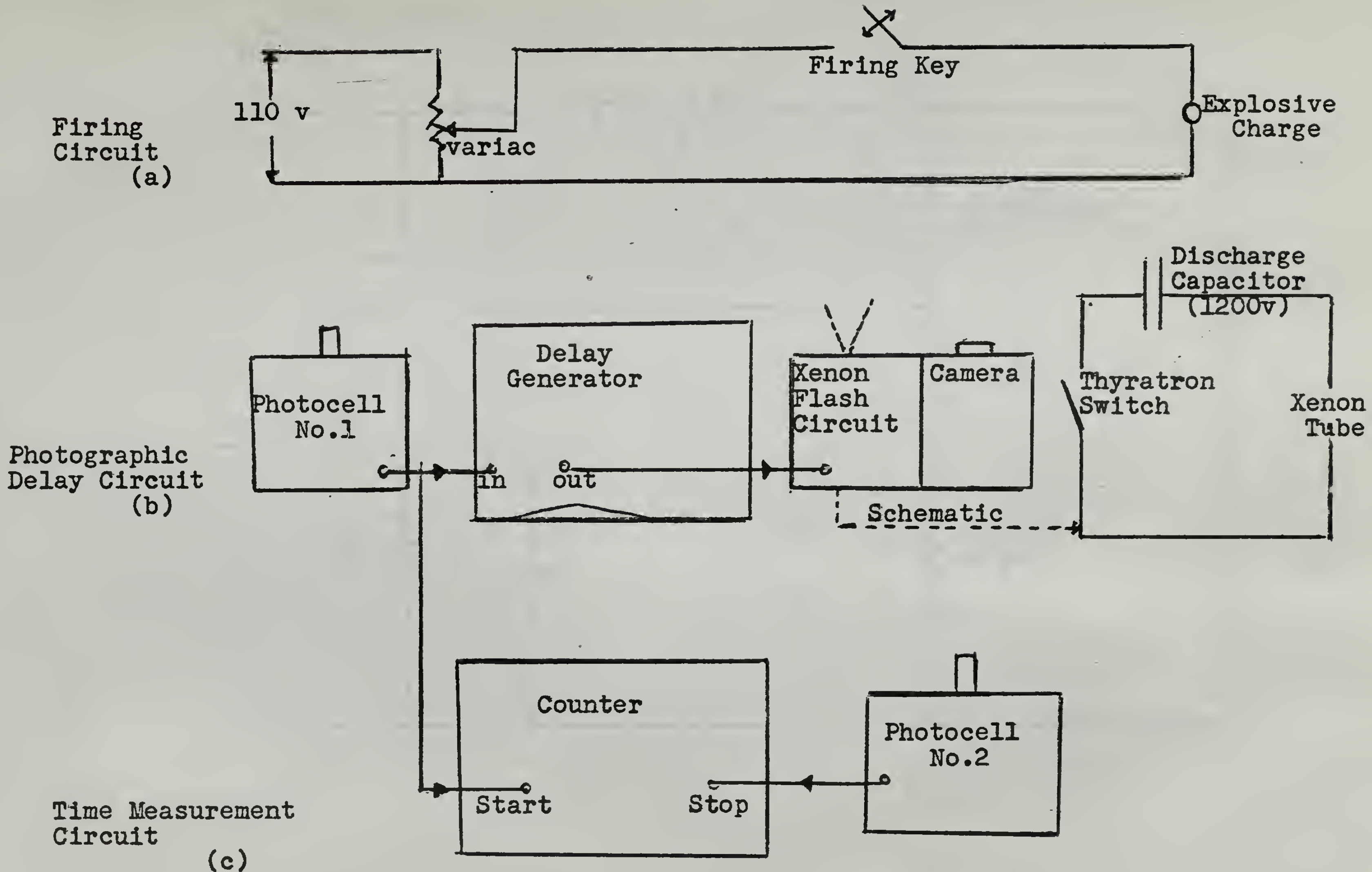
Firing Circuit (a)
110 v
variac
Firing Key
Explosive Charge
Photographic Delay Circuit (b)
Photocell No.1
Delay Generator
in
out
Xenon Flash Circuit
Camera
Schematic
Discharge Capacitor (1200v)
Thyratron Switch
Xenon Tube
Time Measurement Circuit (c)
Counter
Start
Stop
Photocell No.2

Figure 3

[illegible]

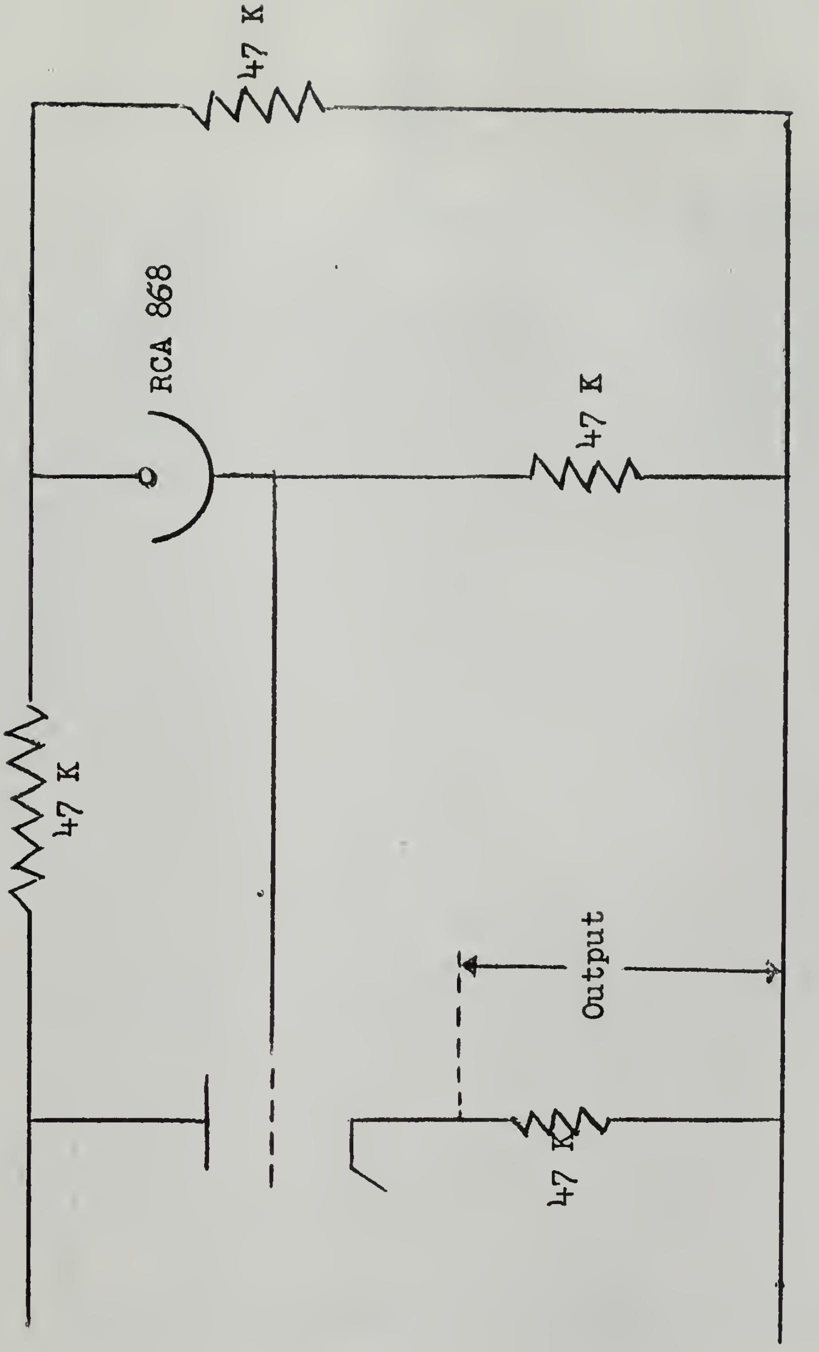

Figure 4

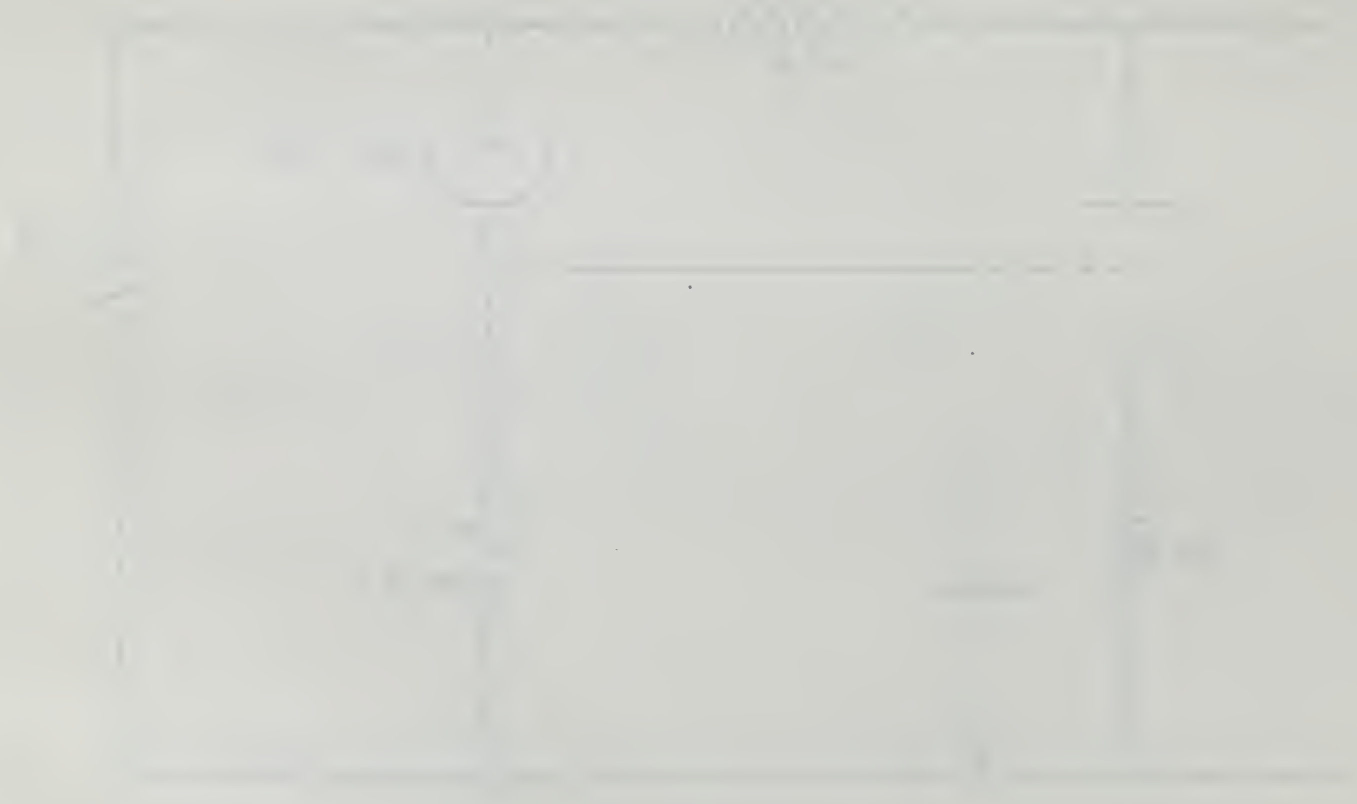

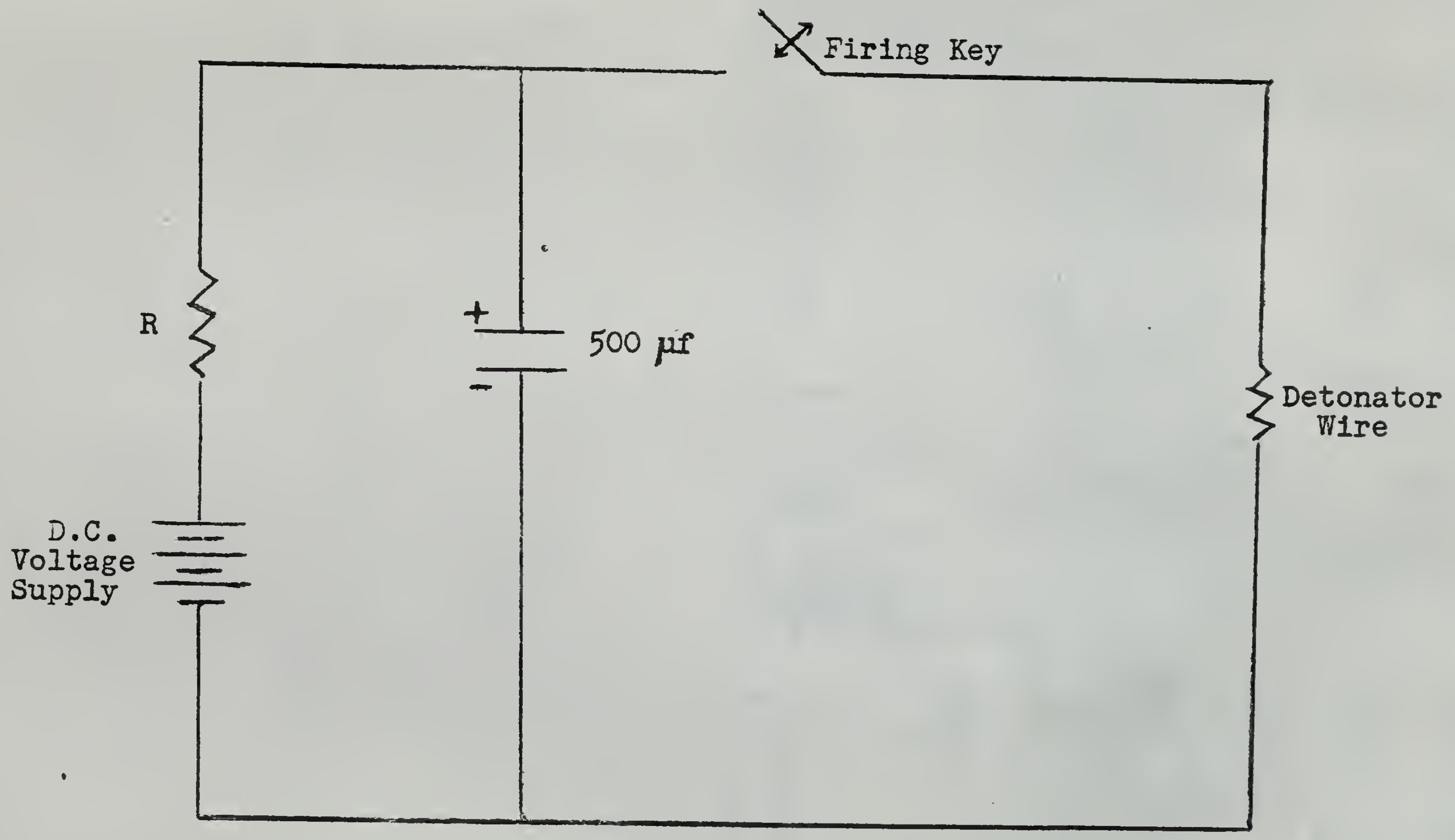

Figure 5

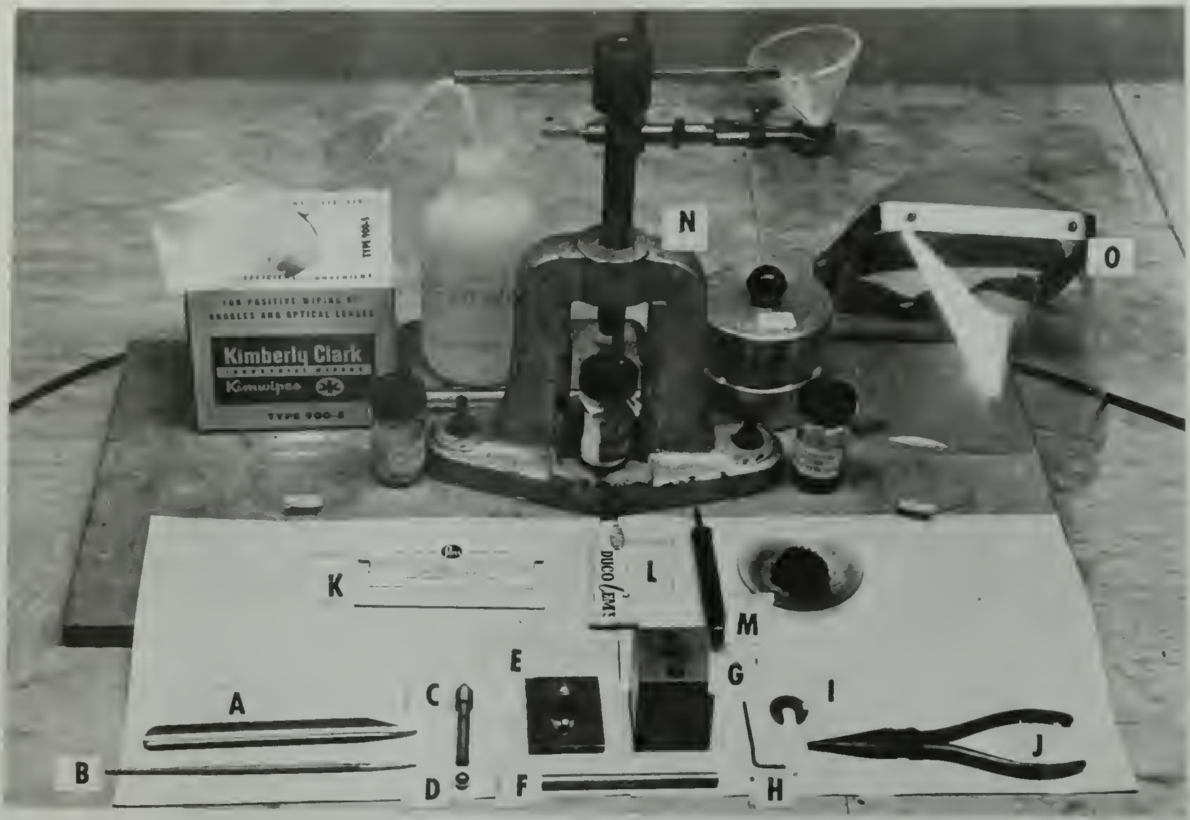

Figure 6

A. Spatula

B. Square ended brush

C. Die Plunger

D. Ball bearing

E. Die Base

F. Brass plunger

G. Die body

H. Allen wrench

I. Stop collar

J. Needle-nose pliers

K. Ni-chrome wire

L. Duco Cement

M. Powdered graphite

N. Press

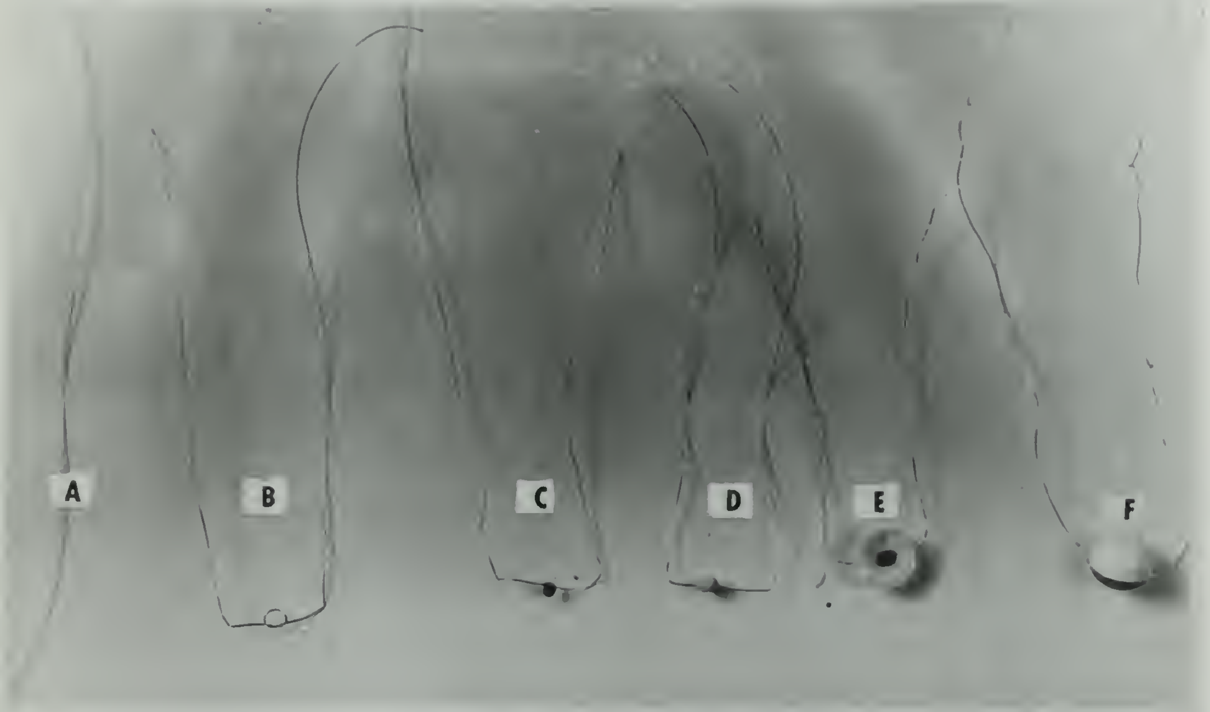

Figure 7

A. Ni-chrome detonator wire

B. Bent wire with loop

C. Styphnate bead on wire

D. Azide bead on wire (completed detonator)

E. Cross-section of charge

F. Complete charge

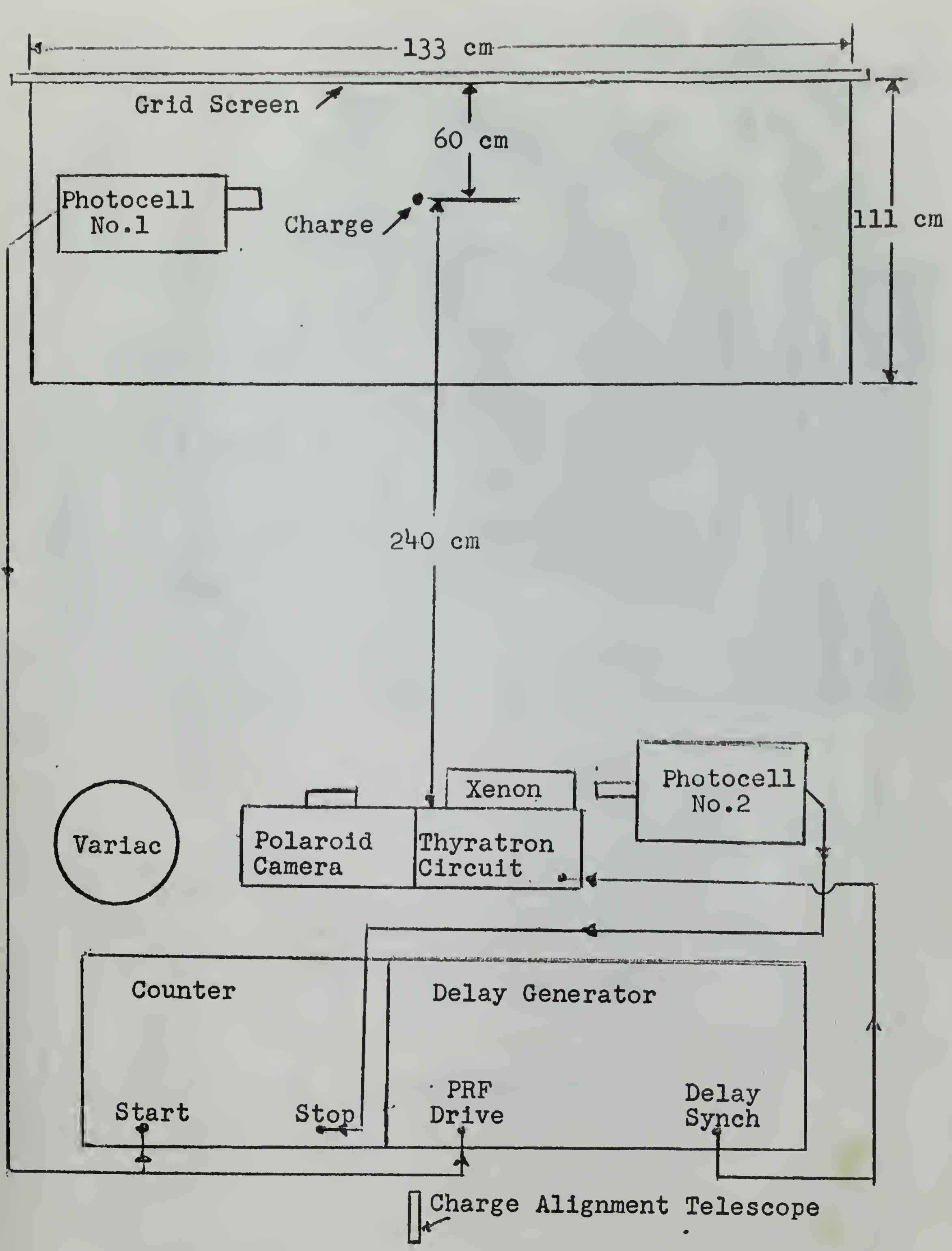
133 cm
Grid Screen
60 cm
111 cm
Photocell No.1
Charge
240 cm
Xenon
Photocell No.2
Variac
Polaroid Camera
Thyratron Circuit
Counter
Delay Generator
Start
Stop
PRF Drive
Delay Synch
Charge Alignment Telescope

Figure 8

[illegible]

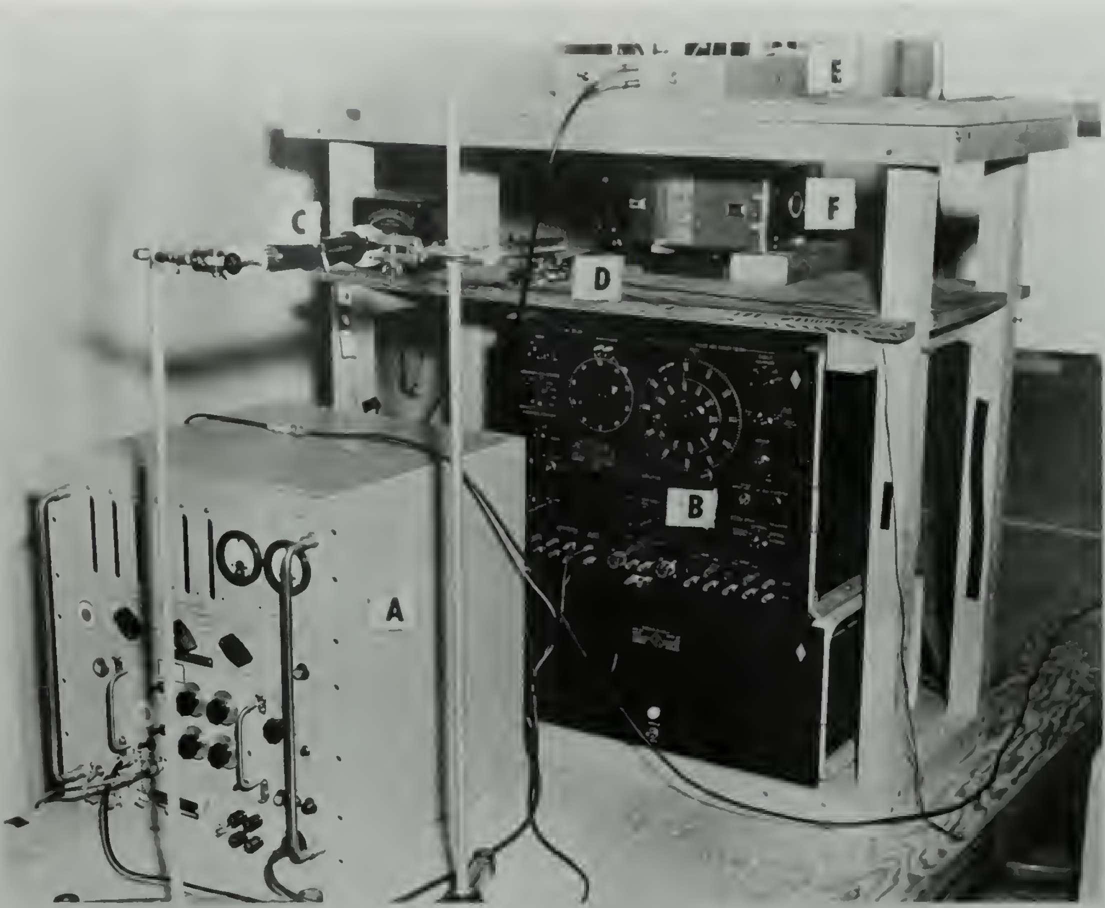

Figure 9

A. Counter

B. Delay generator

C. Telescope (for optical alignment)

D. Firing key

E. Xenon flash-tube electronic components

F. Polaroid camera

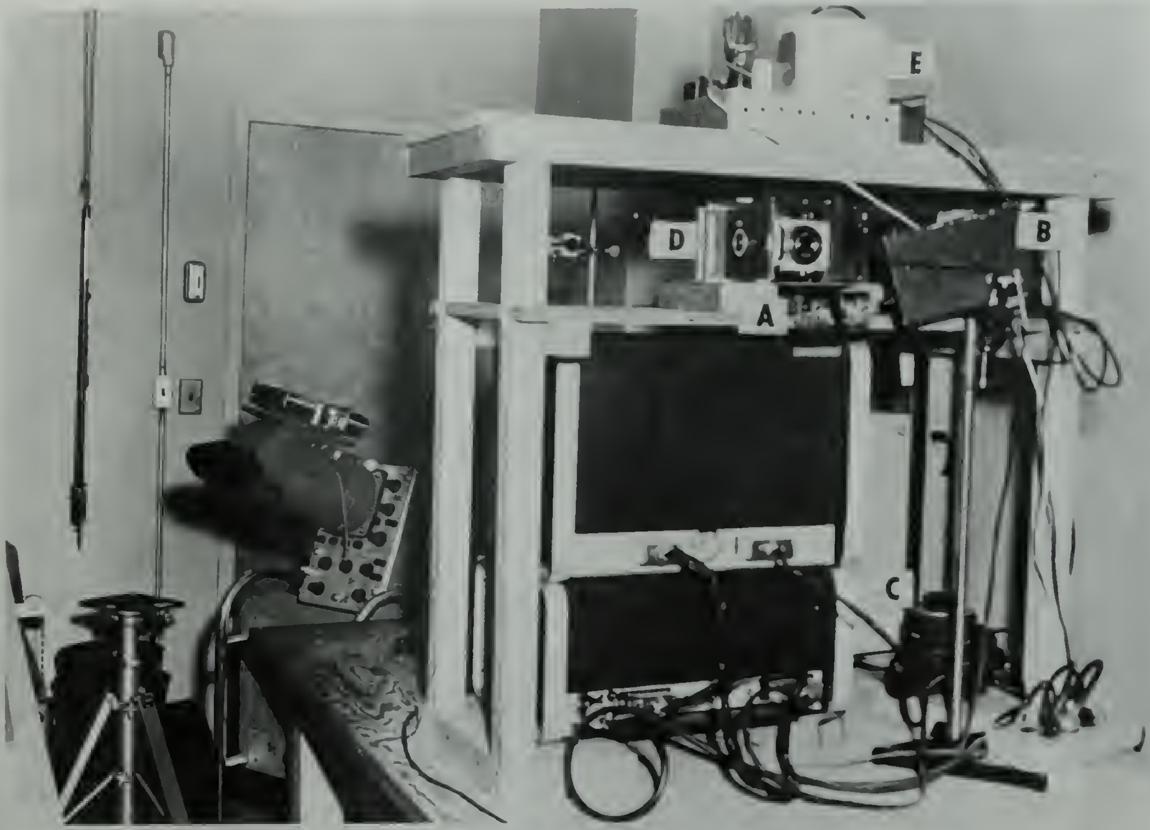

Figure 10

A. Flash tube mount

B. Photocell unit No. 2

C. Variac

D. Polaroid camera

E. Xenon flash tube electronic components

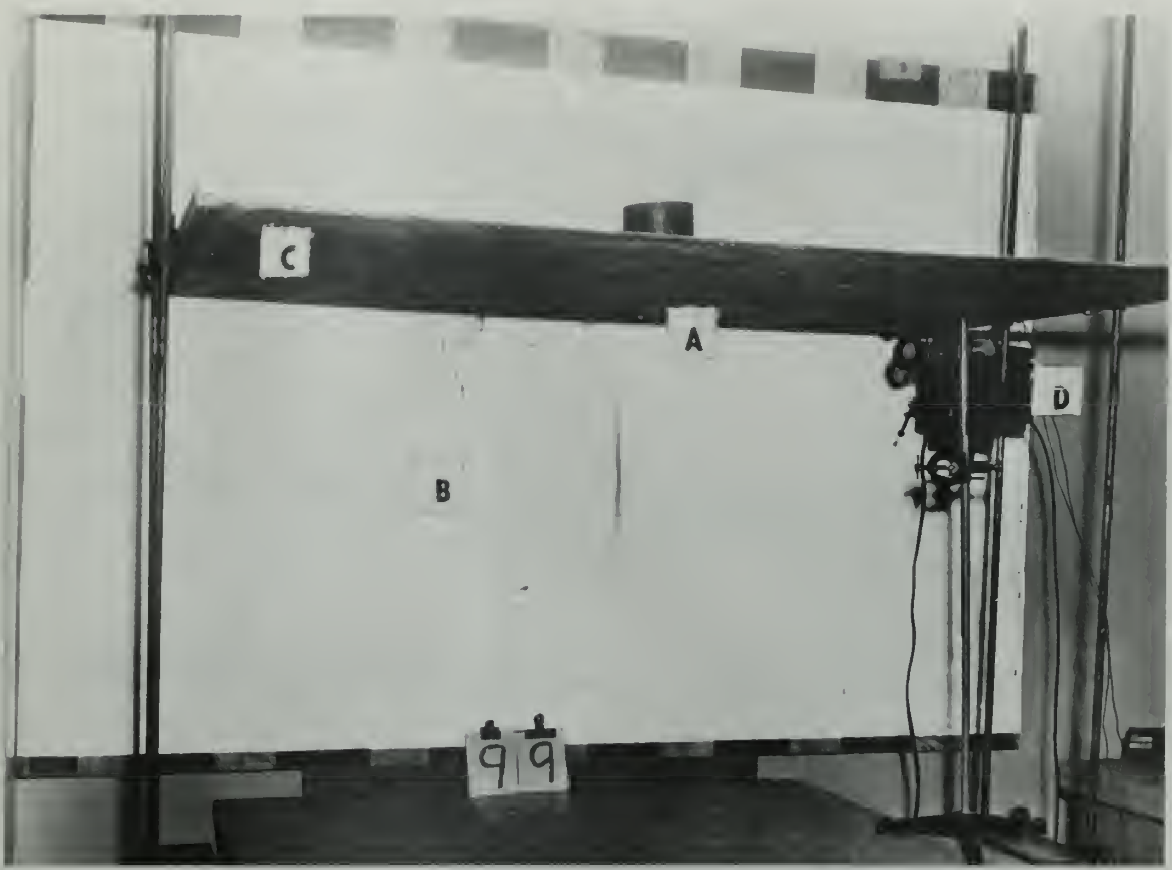

Figure 11

A. Suspended charge

B. Grid Screen

C. Blast table

D. Photocell unit No. 1

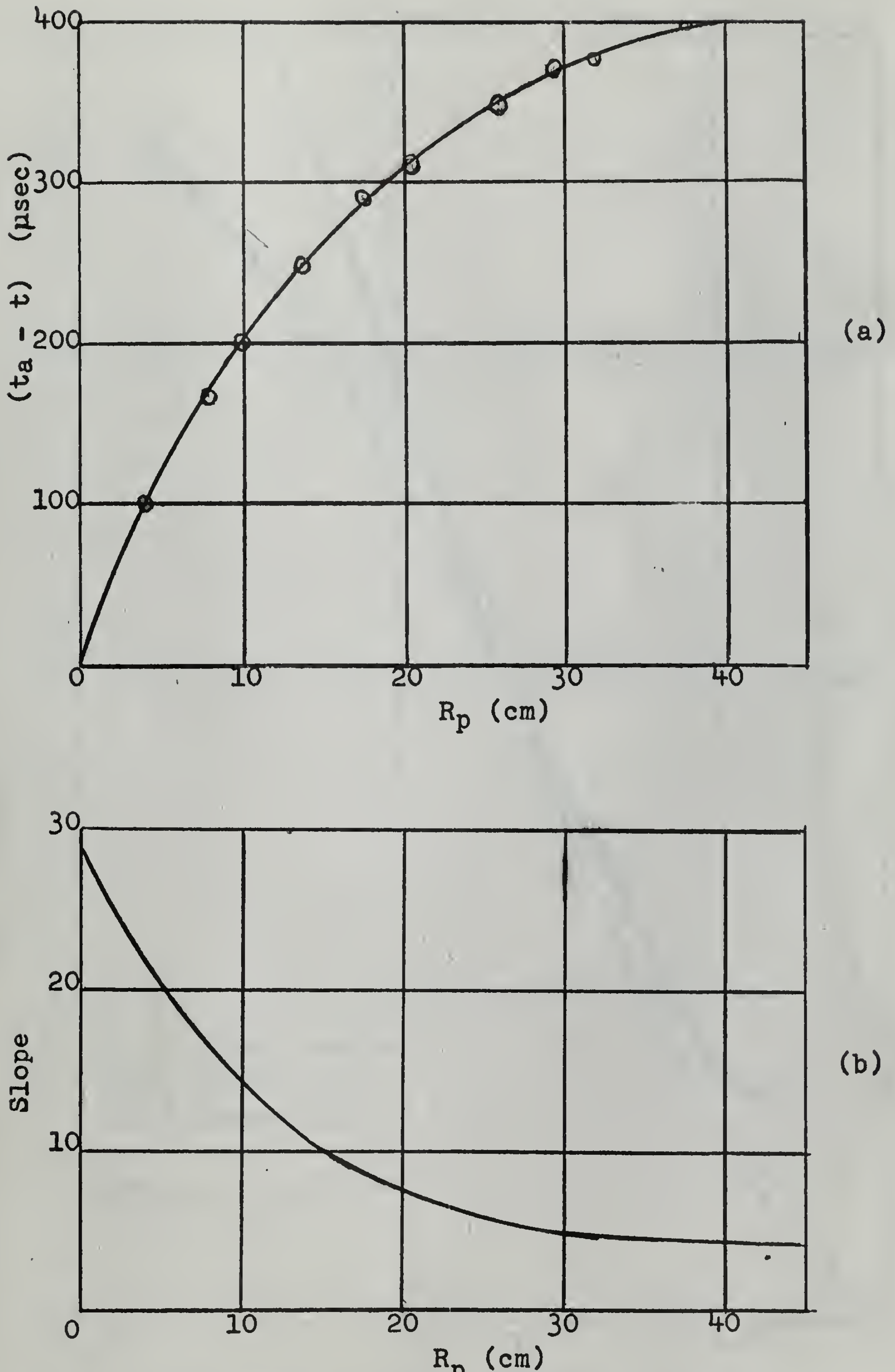
400
300
200
100
0
10
20
30
40
$(t_a - t)$ (μsec)
R_p (cm)
(a)
30
20
10
0
10
20
30
40
Slope
R_p (cm)
(b)

Figure 12

[illegible]

[illegible]

[illegible]

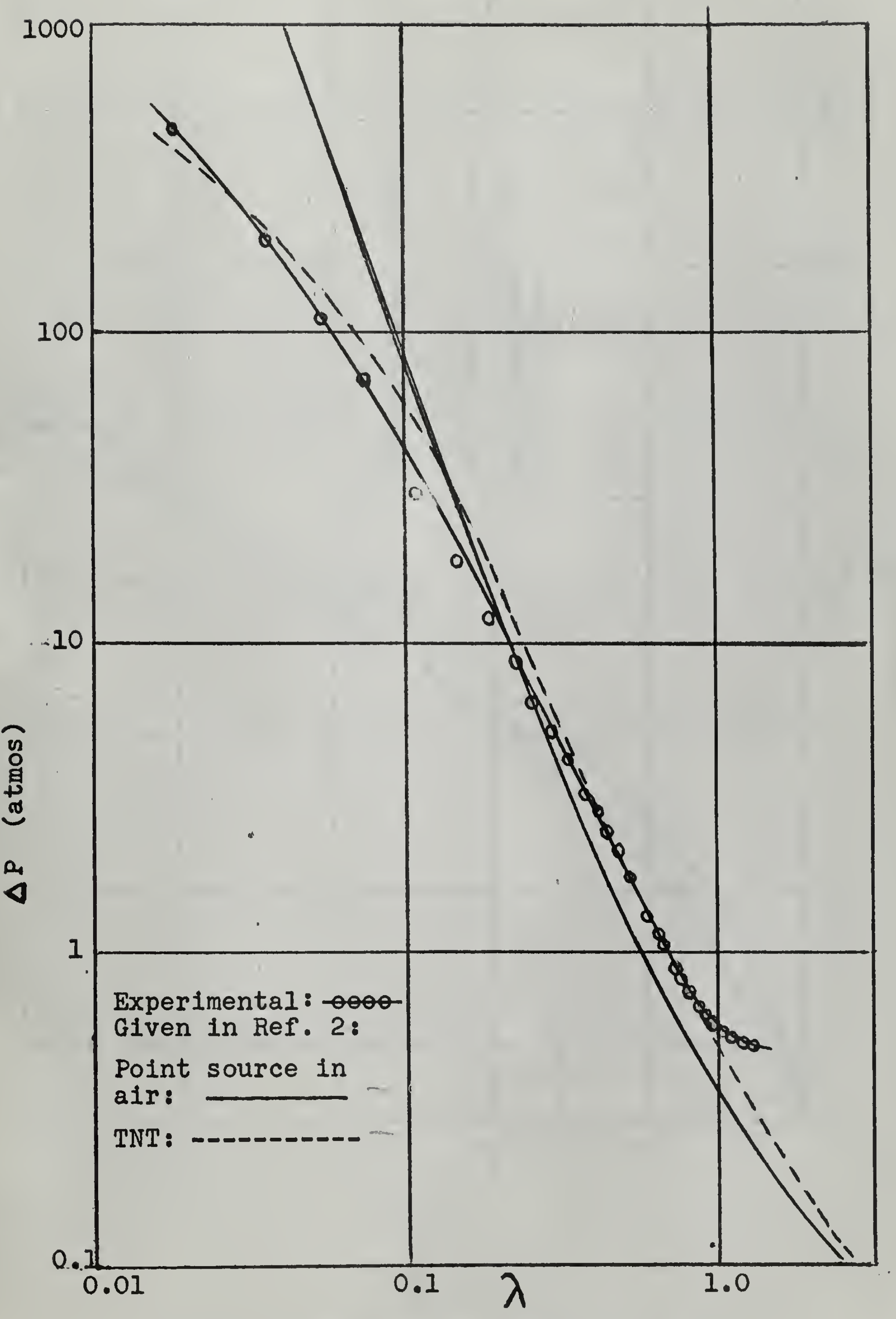

PEAK OVERPRESSURE vs. REDUCED RADIUS

Figure 13

[illegible]

[illegible]

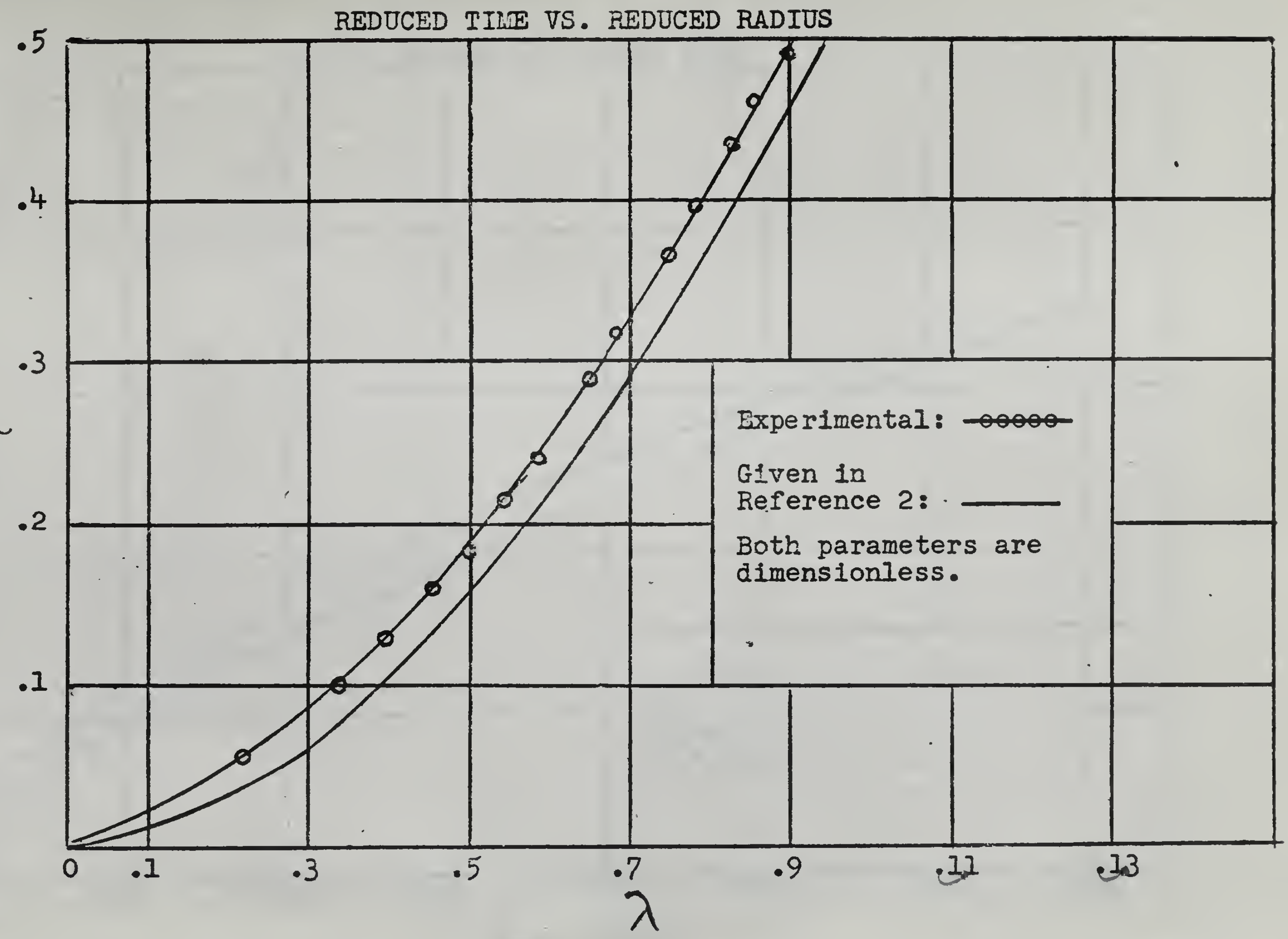
REDUCED TIME VS. REDUCED RADIUS
.5
.4
.3
.2
.1
τ
0
.1
.3
.5
.7
.9
.11
.13
λ
Experimental: -ooooo-
Given in Reference 2: ———
Both parameters are dimensionless.

Figure 14

SCALED RADIUS VS. SCALED TIME

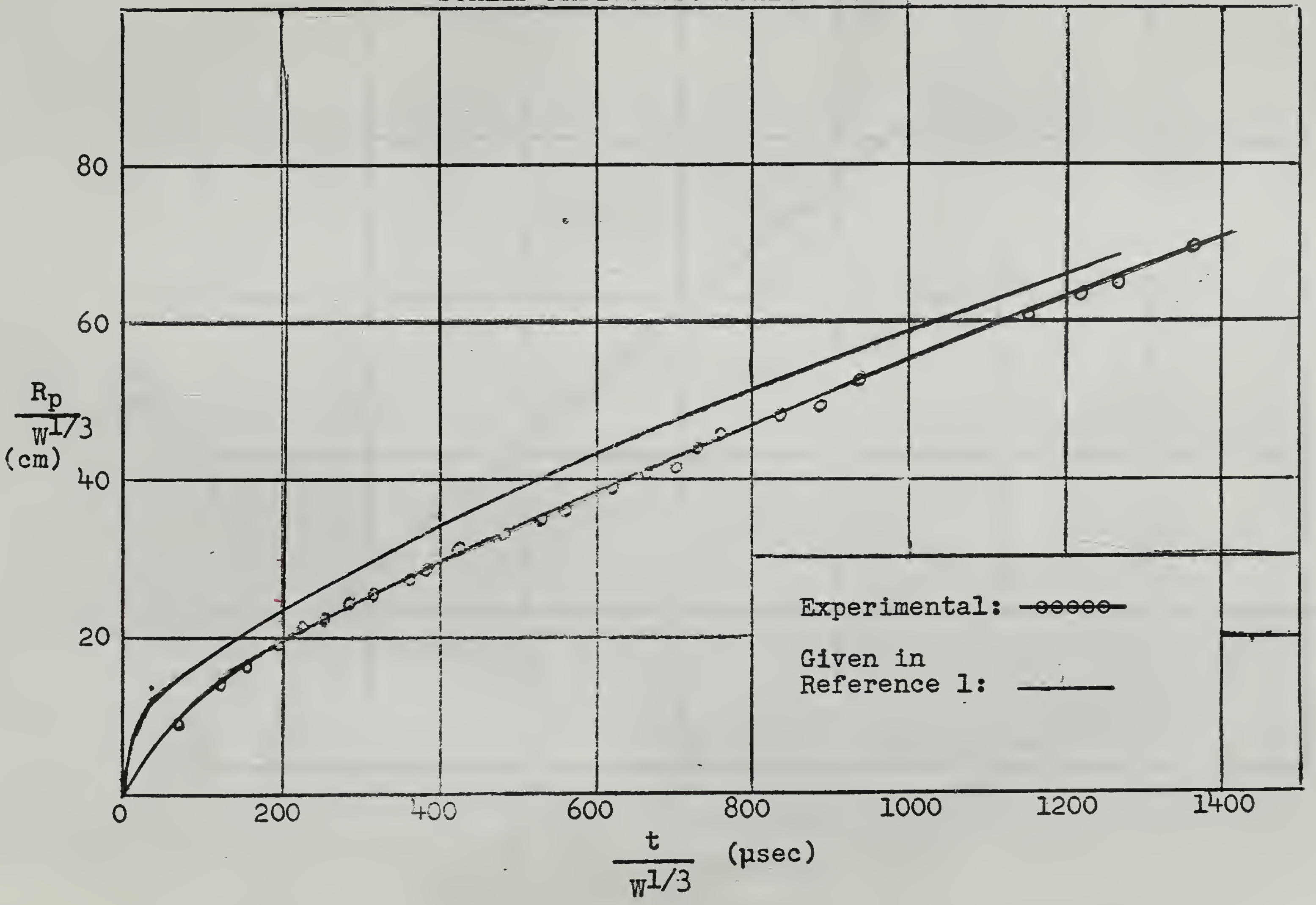

Figure 15

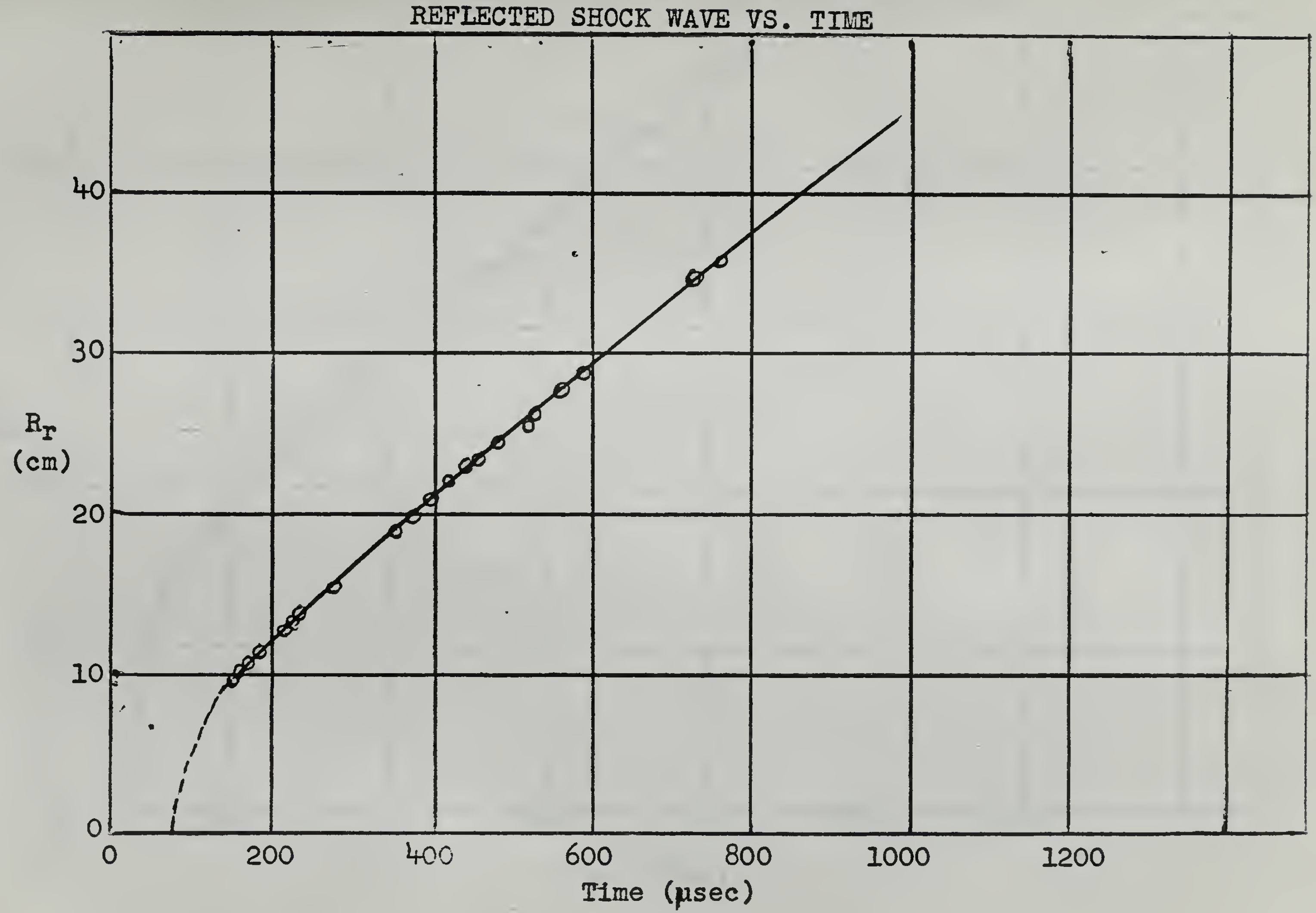
REFLECTED SHOCK WAVE VS. TIME
R_r
(cm)
40
30
20
10
0
0
200
400
600
800
1000
1200
Time (µsec)

Figure 16

DISTANCE OF MACH STEM FROM GROUND ZERO VS. TIME

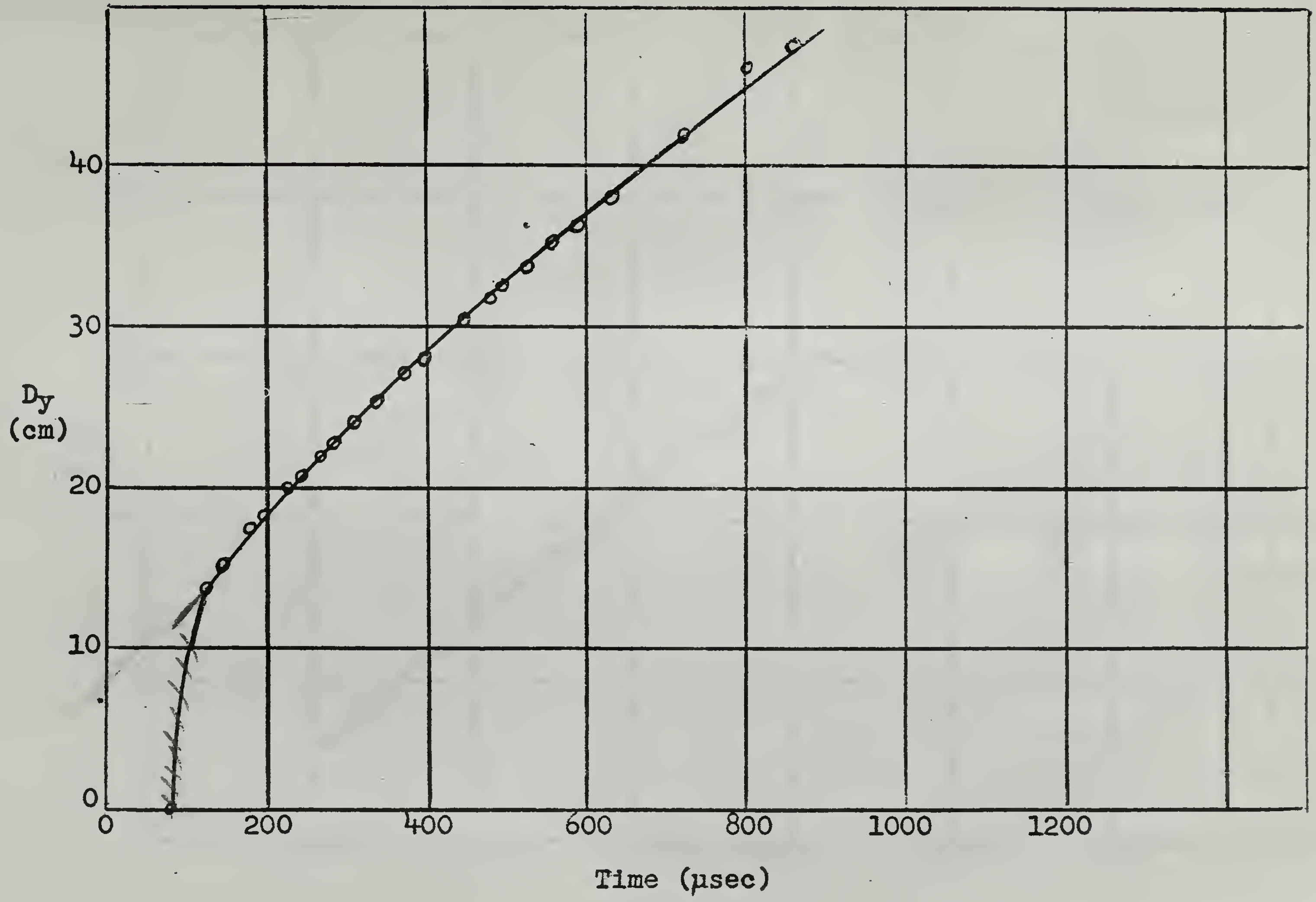

Figure 17

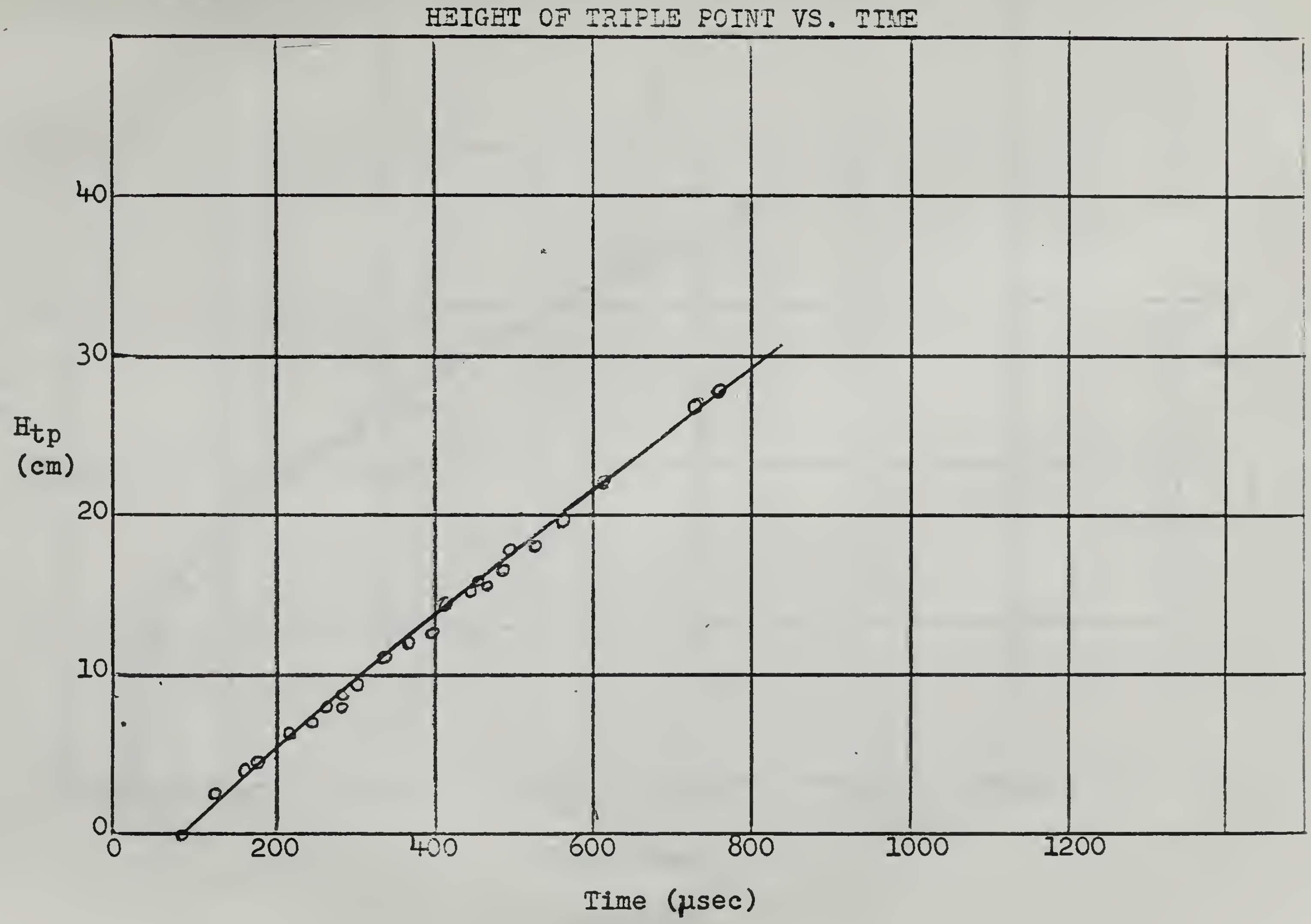
HEIGHT OF TRIPLE POINT VS. TIME
H_{tp}
(cm)
40
30
20
10
0
0
200
400
600
800
1000
1200
Time (µsec)

Figure 18

DISTANCE OF TRIPLE POINT FROM GROUND ZERO VS. TIME

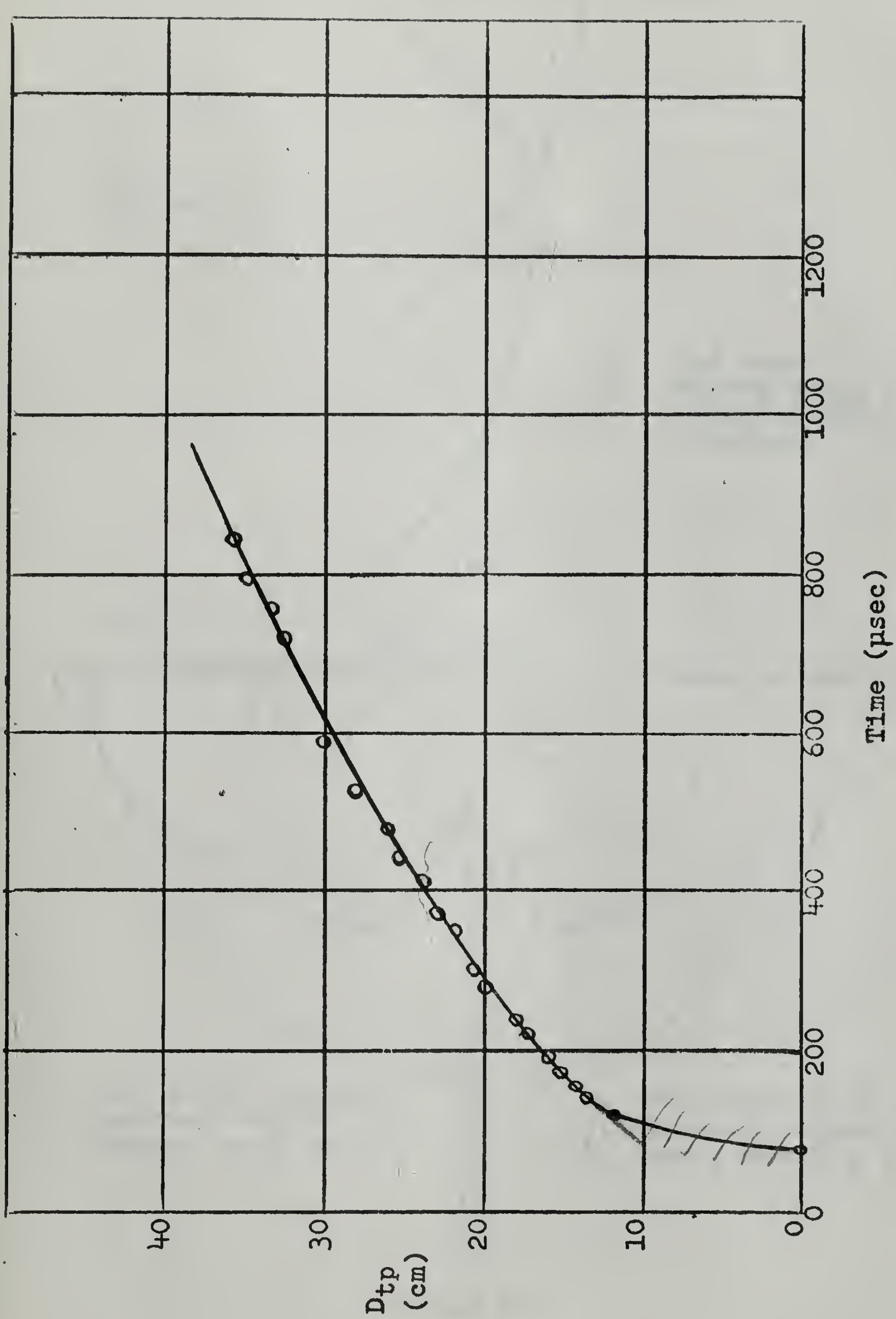

Figure 19

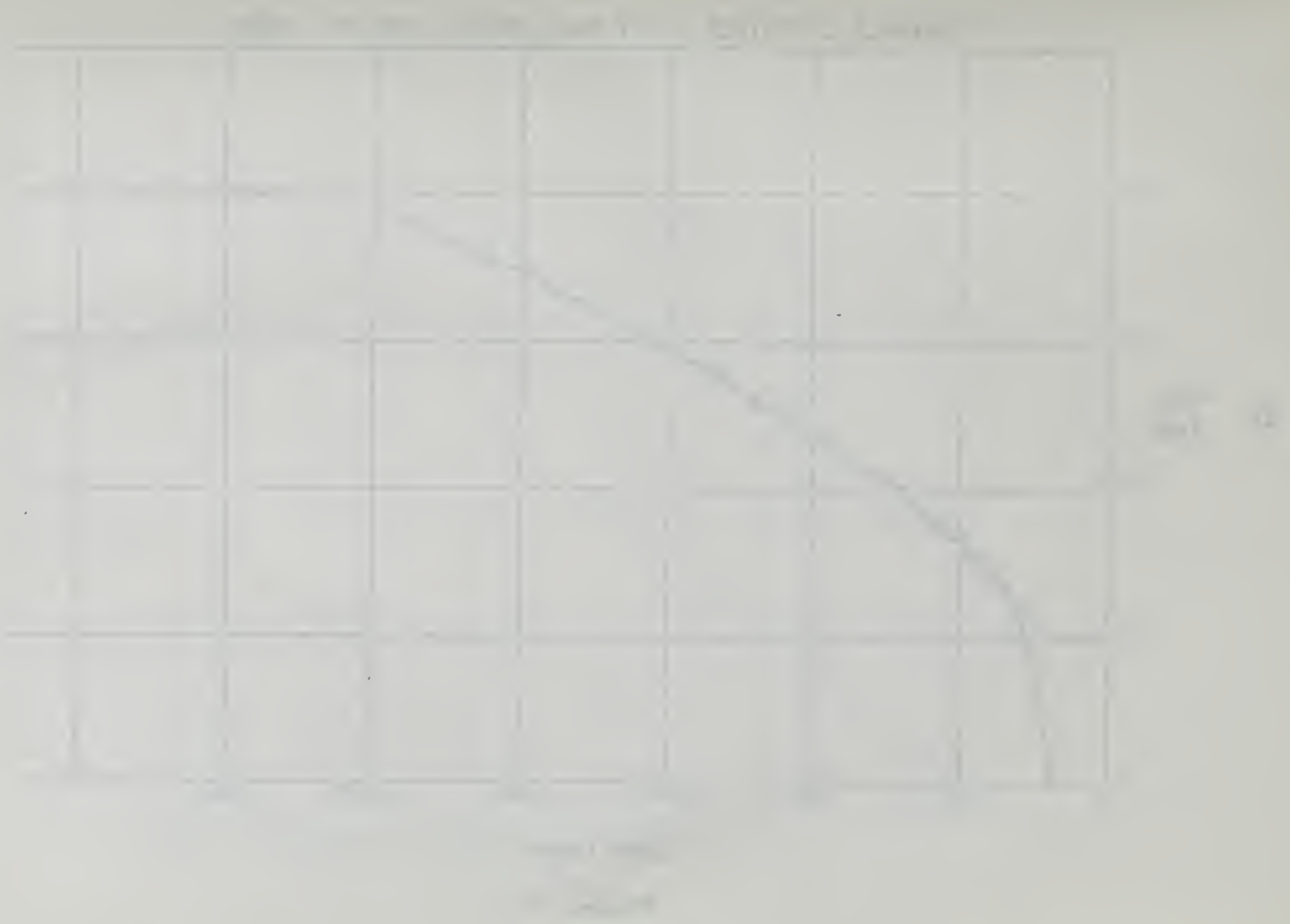

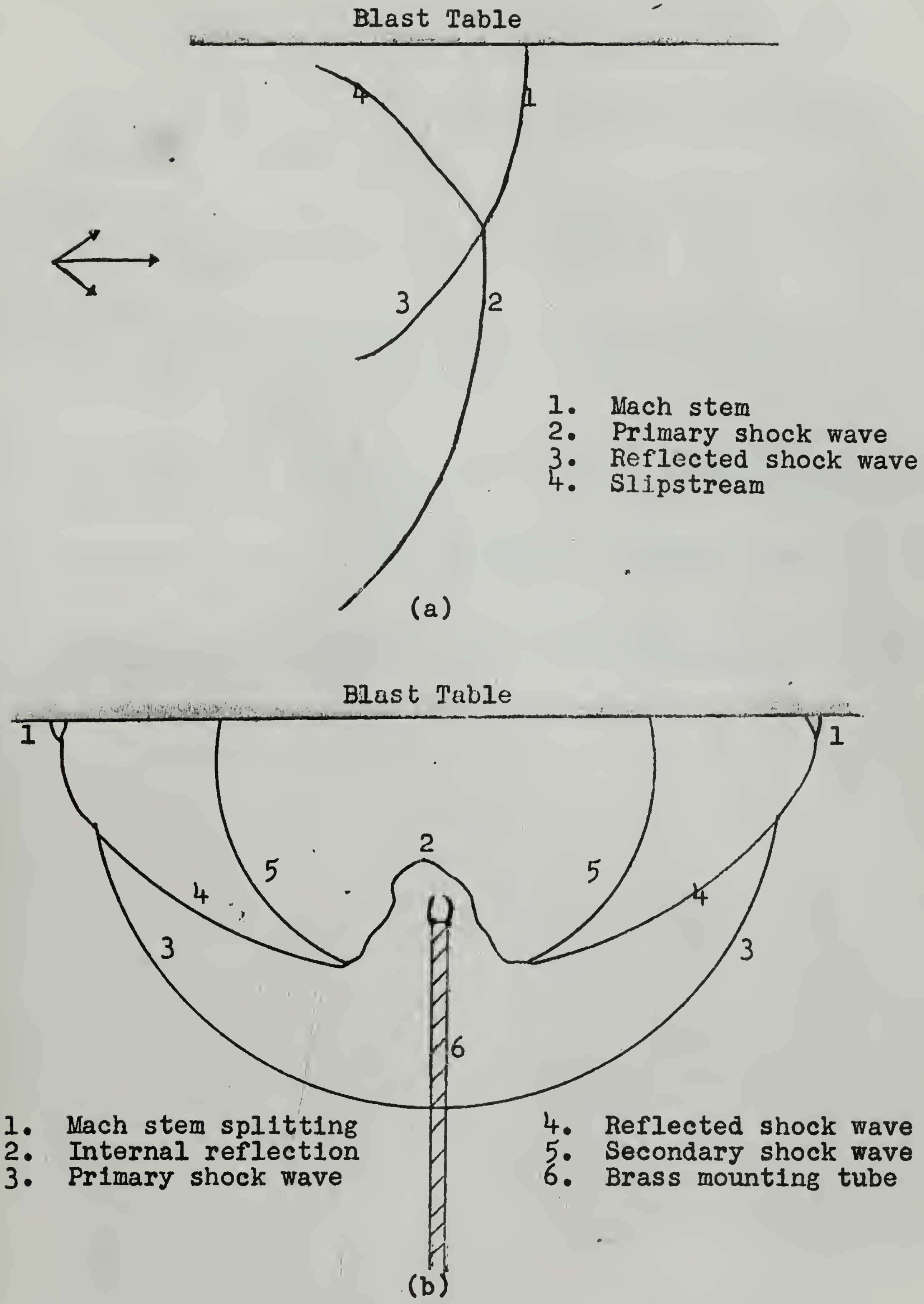Blast Table
1
4
3
2
1. Mach stem
2. Primary shock wave
3. Reflected shock wave
4. Slipstream
(a)
Blast Table
1
1
2
5
5
4
4
3
3
6
1. Mach stem splitting
2. Internal reflection
3. Primary shock wave
4. Reflected shock wave
5. Secondary shock wave
6. Brass mounting tube
(b)

Figure 20

REFERENCES

1. Wilson, P. W. and Treat, C. J., Photographic Investigation of Air Shock Phenomena from Decigram Charges, Thesis W641, U. S. Naval Postgraduate School, 1959

2. Brode, H. L., A Calculation of the Blast Wave from a Spherical Charge of TNT, U. S. A. F. Project Rand, RM-1965, 21 August 1957. [illegible]

3. Kinney, G. F., Blast and Shock Tables for Explosions in Air, U. S. Naval Ordnance Test Station NOTS 1061, NAVORD Report 3458, 11 March 1955. [illegible]

4. Hoffman, A. J. and Mills, S. N., Jr., Air Blast Measurement about Explosive Charges at Side-On and Normal Incidence, Ballistic Research Laboratory Report No. 988, July 1956. U 27,438 [illegible]

5. Tomlinson, W. R., Jr., as revised by Sheffield, O. E., Properties of Explosives of Military Interest, Picatinny Arsenal, Technical Report No. 1740, Revision 1, April 1958. U 29191

6. Glasstone, S. (ed), The Effects of Nuclear Weapons, United States Atomic Energy Commission, June 1957.

7. Edgerton, H. E., Shock Wave Photography of Large Subjects in Daylight, Review of Scientific Instruments, Feb., 1958.